NASA

Technical Memorandum 86159

MAGNETIC PROPERTIES OF JUPITER'S TAIL AT DISTANCES FROM 80-7500 JOVIAN RADII

M. L. Goldstein, R. P. Lepping and
E. C. Sittler, Jr.

SEPTEMBER 1984

National Aeronautics and
Space Administration

Goddard Space Flight Center
Greenbelt, Maryland 20771

MAGNETIC FIELD PROPERTIES OF JUPITER'S TAIL AT DISTANCES FROM 80 - 7500 JOVIAN RADII

M. L. Goldstein

R. P. Lepping

and

E. C. Sittler, Jr.

Laboratory for Extraterrestrial Physics
NASA/Goddard Space Flight Center
Greenbelt, MD 20771

Abstract. A detailed study of the magnetic field data from both Voyagers 1 and 2 has revealed several interesting properties of the near and distant Jovian magnetotail. During the first encounter, as Voyager 1 passed between 80 and 140 R_J from Jupiter in the near tail, the spacecraft was almost entirely in the northern lobe magnetic field. At this time we find that the field lines are slightly twisted by the rotation of the planet into a right-handed helix with pitch angle of about 2° - 3°. The frequency spectrum of magnetic fluctuations in this region cannot be characterized by a power law and does not appear to be turbulent. Some suggestion of a continued tendency of the magnetic field in the distant magnetotail to twist in a right-hand sense in the northern lobe and in a left-hand sense in the southern lobe is found as far as 7500 R_J downstream in Voyager 2 data; however, the evidence is not very strong. At nearly 7000 R_J when the spacecraft was apparently in the magnetosheath near the tail magnetopause, a 5.3 hour periodicity in the magnetic field data is seen, similar to fluctuations observed earlier in the near planet magnetosheath. The magnetic spectra of the distant tail encounters from 6000 - 7500 R_J have power law indices of $f^{-5/3}$ identical to the index of the solar wind magnetic field spectra at these distances. It is possible that the distant tail magnetic fields have become turbulent, or that solar wind fields from the magnetosheath have diffused into the tail. The distant tail spectra from Voyager 2 are compared with similar spectra obtained from Voyager 1 when it was in near radial alignment with Voyager 2. Although the gross properties of the tail and solar wind fields in most respects differ considerably, the shape and power levels of the spectra of the magnetic fluctuations are very similar, especially between 10^{-4} and 10^{-3} Hz. At lower frequencies (10^{-5} to 10^{-4} Hz) the spectra of magnetic helicity do differ.

1. Introduction

The Voyager 1 and 2 encounters with Jupiter and their subsequent trajectories to Saturn have provided a unique opportunity to study the Jovian magnetotail both close to the planet and in a region extending to beyond Saturn's orbit. The presence of a Jovian magnetotail was first reported by Ness et al. [1979a,b,c]. A study of the "near" tail (out to 200-300 R_J) and its associated current sheet was carried out by Behannon et al. [1981]. It was expected, however, that the Jovian magnetotail might extend to beyond Saturn's orbit [Scarf, 1979; Grzedzielski et al., 1980]. The near alignments of Jupiter, Saturn, and Voyager 2 in 1981 provided an opportunity to search for the existence of the Jovian magnetotail as Voyager 2 approached Saturn. Evidence that Voyager 2 had encountered the tail upstream of Saturn was first discovered in the plasma wave and plasma data from Voyager 2 and reported by Kurth et al. [1981] and Scarf et al. [1981]. Later, signatures of penetration into the distant tail were found in the magnetometer data [Lepping et al., 1982]. A complete description of these encounters with the distant tail can be found in Kurth et al. [1982] and Lepping et al. [1983a].

The initial motivation for the present study was the observation by Lepping et al. [1983a] that in the central or "core" regions of the tail the plasma densities reached the very low values of $n \approx 10^{-3}$ particles/cm^3 at times when the magnitude of the magnetic field was relatively low or near minimum. The net plasma and magnetic field pressures within the core appear insufficient to balance the external pressures. Although several explanations for this apparent imbalance are possible, including the existence of a hot plasma population not seen in the PLS thermal plasma experiment [Kurth et al., 1982], Lepping et al. [1983b] suggested the possibility that the

rotation of Jupiter would twist the magnetic fields in opposite directions in the two lobes of the tail and add a centrifugal pressure term to the pressure balance equation.

That magnetic fields in planetary magnetotails might be twisted into helices by the combination of the solar wind interaction at the magnetopause coupled with planetary rotation has been suggested for the earth's magnetosphere [Dessler and Juday, 1965], and for Uranus [Siscoe, 1975; Hill et al., 1983]. Our search for such field twists in the Jovian tail is based on techniques developed by Matthaeus et al. [1982] and Matthaeus and Goldstein [1982a] for determining the magnetic helicity of the fluctuating magnetic fields. We have been able to identify several interesting features of the far Jovian tail, including some evidence for helical twists. For example, rather close to Jupiter (80 - 140 R_J), the magnetic field is indeed twisted in the expected sense, but the degree of twist is slight; i.e., the pitch of the helical field is approximately 2° - 3°. Evidence of twisting is also seen in one penetration into the distant tail at 7500 R_J, but earlier, at a distance of about 6500 R_J, no discernible ordered twisting of the field is evident.

Our analysis of the four most prominent Voyager 2 encounters with the tail have revealed additional features, many of them unexpected. At nearly 7000 R_J a series of oscillations in the magnitude and components of the magnetic field corresponds to a period of 5.3 hours which may be related to the 10 hour rotation of Jupiter [Lepping et al., 1981]. A striking feature of all four of these far-tail intervals is the fact that once inside the tail, as opposed to the magnetosheath, the magnetic fields are fairly well ordered. The average direction of $\underline{B}$ tends to lie either parallel to the radial direction when the spacecraft is in the northern lobe, or anti-parallel to the radial direction when the spacecraft is in the southern lobe.

In the distant tail a spectrum of fluctuations is superimposed on this ordered field that resembles an inertial range of Kolmogoroff turbulence with a power law index of $f^{-5/3}$. Whether this turbulent spectrum is due to internal dynamical stirring of the medium arising from "substorms" or magnetic reconnection, external forcing of the tail by the solar wind, simple leakage of solar wind or magnetosheath fields into the tail, or some other cause, cannot be determined from our results alone. A comparison of these Voyager 2 data with solar wind fields measured at Voyager 1 some five days later for each of the four cases demonstrates that, although there is often a striking similarity in the magnitude and shape of these Voyager 2 tail spectra and Voyager 1 solar wind power spectra, the magnetic helicity spectra are often distinct.

In the next section we review the spacecraft trajectories and give an overall review of the magnetic field data in the intervals we analyzed. This includes the region close to Jupiter between 80 - 140 R_J that was probed by Voyager 1, the four prominent Voyager 2 distant tail encounters between about 6000 - 7500 R_J denoted 2, 3, 4, and 5 by Lepping et al. [1983a], as well as two types of control intervals of "solar wind" or magnetosheath data. In the first set of controls, we have estimated the convection time of solar wind plasma and field from the position of Voyager 2 to Voyager 1 and have used that data to reflect the approximate "local" external interplanetary conditions while Voyager 2 was in the far Jovian tail. In a second set of controls, we selected two Voyager 2 time periods some 6000 R_J downstream of Jupiter when Voyager 2 was in the solar wind-like Jovian magnetosheath.

In section 3, we examine the four distant tail encounters and compare them with the corresponding Voyager 1 interplanetary data sets. Additional information can be obtained from a power spectral analysis of both the near

and distant tail intervals. This is given in section 4 where some of the differences between the tail encounters and the power spectra of these same control data sets are discussed. Section 5 contains an analysis of two solar wind or magnetosheath data sets obtained when Voyager 2 was not in the distant tail. We contrast these more "normal" solar wind conditions to those reflected in both the Voyager 2 distant tail encounters and the conditions monitored by Voyager 1 farther downstream. Section 6 contains a discussion and conclusions, and a summary of our results is given in Section 7.

2. An Overview

Some of the features of the magnetic field and thermal plasma of the one near and four distant Jovian tail intervals discussed in this paper have been described by Behannon et al. [1981] and Lepping et al. [1983a], respectively. The reader is referred to those references and to Kurth et al. [1982] for additional details on the general morphology of the Jovian tail, and in particular for a discussion of how the far tail was identified in the data. The first interval of concern occurred following Voyager 1 encounter with Jupiter. The trajectory of that encounter is shown in Figure 1 (adapted from Behannon et al. [1981]). Included is a sketch of the model magnetopause and bow shock positions as described by Lepping et al. [1981]. The day of the year 1979 is also labeled on the trajectory. In Figure 2 we show a plot of the magnetic field components in spacecraft centered heliographic coordinates. In this coordinate system, $\hat{R}$ is along the sun-spacecraft line, positive away from the sun, $\hat{T}$ is perpendicular to $\hat{R}$ and parallel to the sun's equatorial plane, positive in the sense of the sun's rotation, and $\hat{N} = \hat{R} \times \hat{T}$. In the spherical coordinates used in this paper, λ is longitude measured

counterclockwise in the $\hat{R}$-$\hat{T}$ plane ($\lambda = 0°$ for $\underline{B}$ parallel to $\hat{R}$) and δ is latitude measured with respect to the $\hat{R}$-$\hat{T}$ plane (positive for $B_N > 0$). The plot starts at day 69 and ends near the end of day 72, spanning the downstream region from some 80 to 139 R_J. There were no complete current sheet crossings and Voyager 1 remained in the northern lobe of the tail.

It is apparent that although the current sheet is not completely traversed, the rocking of the Jovian current sheet [Behannon et al., 1981] brings the spacecraft down from high latitude lobe fields to the current sheet, and back again, with a periodicity of approximately 10 hours. Note that near the current sheet, large high frequency fluctuations in the components of the field are evident. In this near-planet lobe region outside of the current sheet penetrations, the plasma density is extremely low ($n \simeq 10^{-5}$ particles/cm^3) almost everywhere [Gurnett et al., 1980]. Consequently, in the lobes the Alfvén speed, denoted by V_A and defined by $V_A = B/\sqrt{(4\pi nm)}$, is of order 30 000 km/s for an observed 4.3 nT field. The primary reason for examining this interval, which has already been described in some detail by Behannon et al. [1981], is that if the rotation of Jupiter imparts any large scale helical twist to the field, it should be evident as a right handed twist in the field during the 3 1/2 days Voyager 1 was in the northern lobe.

We can estimate the expected pitch angle of the twisted "helical" field in this near tail region by modeling the helical part of the field, in either lobe, as an Alfvén wave propagating tailward parallel to the tail axis in a very low density plasma that itself has a finite convection speed. It is easy to show that the pitch angle of such a field is approximately given by

$$\alpha = \arctan(2\pi R/\tau V)$$

where R is the radius of one of the tail lobes, τ is the period of the wave, and $V = V_c + V_A$ (V_c is the convection speed of the plasma in the lobe carrying the wave). Here, V_A is the average local Alfvén speed. We assume that the wave results from the twisting of tail field lines that are effectively anchored to the rotating planet with little or no ionospheric slippage. Thus, τ = 9.92 h, Jupiter's rotation period. The plasma density deep in the lobe at a planetocentric distance $d \simeq 85\ R_J$ has been estimated by Gurnett et al. [1980] to be 10^{-5} cm^{-3}. Close to the magnetopause or neutral sheet, however, the density is apparently much higher. We take a value of 4.5 nT for the average magnitude of $\underline{B}$ on days 69 - 72 (cf. Figure 2), which yields $V_A = 31 \times 10^3$ km/s. The convection speed of the lobe plasma is not known, but will be assumed to be zero compared to V_A. On day 71, the radius of the tail lobe $R \simeq 130\ R_J$ as estimated from the model tail magnetopause position (cf. Figure 1). The estimated pitch angle is then $\alpha \simeq 3.0°$. Since the density in this region will vary considerably depending on d and on the particular subregion of plasma (boundary layer, plasma sheet, etc.) [see, Gurnett et al., 1980], V_A and, therefore α, will vary considerably with spatial location in the lobe, but at least near $d \simeq 85\ R_J$, our estimate that $\alpha \simeq 3°$ appears reasonable. In section 4, we will derive an estimate for α using spectral techniques that will constitute an average over the entire time period illustrated in Figure 2.

The remaining encounters we discuss were all with the distant tail and occurred during 1981. At the time of these encounters, Voyager 2 was between 5000 and 9000 R_J from Jupiter and was very close to the sun-Jupiter line. The trajectory of the spacecraft is shown in Figure 3. The plot is in both cylindrical coordinates (top panel) and Jupiter orbital plane coordinates (bottom panel). The X′ axis is aberrated by 1.8° from X to account for

Jupiter's motion in a solar wind flowing at 420 km/s. Hence X' is aligned with the nominal tail axis. The 14° cone represents the region within which all distant tail encounters have been observed, including several post-Saturn Jovian tail encounters (not shown) as identified in Voyager 2 magnetometer data, Plasma Wave Science data (W. Kurth and F. Scarf, private communication), and Planetary Radio Astronomy data (M. Desch, private communication). Tail encounter events K,K,1-8, are those discussed by Lepping et al. [1983a]. Saturn encounter occurs shortly after event 8. Only the most prominent tail encounter events 2-5 will be discussed here. The distance $\rho'_{C.A.}$ refers to the closest approach distance between Voyager 2 and the X' axis. This occurs during the middle of event 4.

An overview of the magnetic field data obtained over the trajectory shown in Figure 3 is plotted in Figure 4. This plot of two-hour average data covers the 130 day period from day 30 to day 160 (1981), corresponding to 6000 to 7500 R_J down the tail (cf. Figure 3). Intervals 2 - 5 are indicated on the plot as are two control intervals denoted A and B. As we shall see, these control intervals differ both qualitatively and quantitatively from the tail encounter intervals. They were also used as control intervals by Lepping et al. [1983a], who determined that they were solar wind-like magnetosheath regions. Our analysis lends support to the conclusion that the distant tail data is very distinct from typical solar wind data.

It is a general feature of this 130 day interval that encounters with the distant tail tend to occur following the field compressions associated with stream interaction regions. The high fields of the interaction regions, in association with the higher total pressure of the solar wind plasma, should tend to *compress the tail and move it away from Voyager 2. Conversely, in* the relatively low pressure of the rarefactions that follow these compres-

sions, the internal pressure of the tail (resulting primarily from the pressure of the magnetic field) causes an expansion that enhances the probability that tail will envelope Voyager 2. Lepping et al. [1983a] have pointed out that this alteration of high and low pressure regions in the solar wind will give the tail boundary a "sausage string" shape and accounts for the approximate 25 day periodicity of tail encounters.

A clearer picture of how the structure of the distant tail differs from normal solar wind plasma conditions could be constructed if one could monitor the solar wind outside the tail at the same time that the tail encounter data was obtained. Because Voyager 1 was nearly aligned with Voyager 2, it is almost possible to achieve this goal. Lepping et al. [1983a] give a general comparison of the two spacecraft positions and data sets. They noted that Voyager 1 data show no indication of penetration into the Jovian tail. However, the spacecraft was only some 16° away from the nominal unaberrated Jupiter tail axis during this time and was approximately 1.6 AU farther downstream. This means that solar wind plasma flowing past the tail near Voyager 2 passed close to Voyager 1 some 5 days later. The alignment of the two Voyagers is not perfect in that Voyager 1 was farther out of the ecliptic plane than Voyager 2.

Two-hour averages of the Voyager 1 magnetic field data for this time period are shown in Figure 5. The general pattern of corotating stream interaction regions seen in Figure 4 is repeated here. The longitude, λ, tends to cluster around either 90° or 270° with more regularity in this data set than was true in Figure 4 where tail encounters tended to cause a rotation of λ from its Parker spiral value to orientations closer to 0° or 180°. If the Voyager 1 data is shifted in time by five days, we can see that during the penetrations of Voyager 2 into the distant tail the local external

solar wind is characterized by low magnetic field magnitudes. It appears that one is indeed in a stream rarefaction region during these distant tail encounters as was inferred from the Voyager 2 data alone. One of the distinguishing features of penetrations into the tail, which we will illustrate in more detail in Figure 6 - 9, is that the magnitude of the solar wind magnetic field is low. It is probably this low field (as monitored by Voyager 1) and the inferred low total plasma pressure (kinetic plus ram pressure) that causes the tail to inflate out to Voyager 2. Once in the tail, the field magnitude gradually decreases further as the neutral sheet is approached. As expected, λ shifts from values near 0° to values near 180° as the spacecraft moves from one lobe into the other. In contrast, when the spacecraft are in the solar wind, λ tends to be close to 90° or 270°.

3. The Distant Tail Encounters

Lepping et al. [1982], in their description of event 2, noted that either of two qualitative models could explain the main signatures of the magnetic field profile near day 50 (1981); a similar description can be applied to some of the other distant tail encounters discussed here. In both models (cf. their Figure 4), they concluded that Voyager 2 first entered the northern lobe field, briefly penetrated into the core of the southern lobe, and then exited through the northern lobe. The main difference between the models was whether, after penetrating into the southern tail lobe, the spacecraft actually retraced its path through the northern tail lobe, or, alternatively, moved through a warped neutral sheet. In the first case the observed magnetic field would represent a symmetry in time, in the second case, the relative motions of spacecraft and tail would produce a magnetic

field signature that is symmetric in space. The magnetic field data and the PLS plasma density and speed for event 2 is plotted in Figure 6a. Similar interpretations are consistent with the brief periods of $\lambda \simeq 180°$ in Figure 7a for event 3. Event 4 (cf. Figure 8a) is rather unique and will be described in more detail below. A somewhat different sequence of events occurred during event 5 (Figure 9a) in that Voyager 2 first encountered the southern lobe ($\lambda \simeq 180°$), remained there for some four days, and then passed into the northern lobe ($\lambda \simeq 0°$). During the following four days there were brief excursions back into the southern lobe. The plasma data displayed in Figures 6a, 7a, 8a, and 9a were derived from the moment estimates of the ion density and speed which were computed by integrating over the complete ion spectra as described in Kurth et al. [1982]. Whenever the density falls below about $10^{-2}/cm^3$, the speed determination as computed from the moments is of questionable validity. Therefore, speeds are shown only when the ion densities are greater than about $10^{-2}/cm^3$. The cross-hatched regions in the density plots denote the lowest density "core" regions of the tail ($n \leq 10^{-2}/cm^3$) determined from the PLS data as tabulated in Table 2 of Kurth et al. [1983]. In contrast, the regions marked "core" on the panel containing magnetic field magnitude are derived from PWS data and represent times when there was an abrupt intensification in the intensity of plasma continuum radiation coupled with a drop in the low-frequency cutoff. These times are listed in Table 1 of Kurth et al.

In panels b of Figures 6 - 9 we have plotted the time shifted solar wind data as recorded by Voyager 1. Only magnetic field data is shown because the PLS instrument on Voyager 1 had ceased functioning by this time. A comparison between the tail and solar wind data for event 2 indicates some interesting similarities. The magnitude of $\underline{B}$ in panels (a) and (b) are

similar, suggesting that to some extent the tail lobe fields are responding to external solar wind dynamics. However, at Voyager 1 the interplanetary field at 10 AU is wound into a fairly tight Parker spiral ($\lambda \simeq 90°$). In contrast, at Voyager 2, λ is usually closer to 0° or 180° except when the spacecraft approaches the core of the tail and is near the neutral sheet. Thus, the large scale structure of a planetary magnetotail is preserved in this data set at more than 6000 R_J from Jupiter. Lepping et al. [1982] noted that if Voyager 2's passage through the tail was approximately a straight path through a warped current sheet (the space symmetry model), then there had to be an interplanetary magnetic sector boundary crossing while Voyager 2 was in the tail. In panel (b), one can see that λ remains near 90° throughout this time period. Therefore, no interplanetary sector crossing was seen by Voyager 1 at this time. Thus, it appears that the space-symmetry model is not viable, which reenforces the belief expressed by Lepping et al. [1982] that the time-symmetry model is a more accurate one. The discussion above concerning the expansion and contraction of the tail to the position of the spacecraft is also consistent with the time-symmetry model.

Event 3 (Figure 7) has been discussed by both Kurth et al. [1982] and Lepping et al. [1983a]. The disappearance of continuum radiation before Voyager 2 left the low density tail led Kurth et al. to suggest that this encounter may be one in which the tail has actually disconnected from Jupiter. Kurth et al. [1982] pointed out that the disconnection would probably be associated with a sector crossing, in analogy with plasma tail disconnection events in comets. The data at Voyager 1 (Figure 7b) show that a sector crossing did occur in the solar wind during event 3. In general there is little detailed correspondence between the fields measured by Voyager 2 and the corresponding region seen later at Voyager 1 at day 81.

The story is further complicated because at Voyager 1 the first few days of this interval included the trailing edge of a high speed stream (cf. Figure 5) which has not been included in Figure 7b. This stream has probably compressed and distorted some of the field patterns originally present in the vicinity of Voyager 2.

The fourth event (Figure 8) is one in which for the first 6 days all components of $\underline{B}$, and especially λ, are generally similar at both spacecraft. At the time of this event, Voyager 2 is closest to the aberrated position of the axis of the Jovian tail, the point marked $\rho'_{C.A.}$ in Figure 3. One might imagine that the similarity in the fields arises because Voyager 1 had also encountered the tail, but the complete absence of continuum radiation and the fact that λ is either close to 90° or 270° eliminates that possibility. Furthermore, from Figures 5 and 8b, one can see evidence for a large loop or magnetic cloud [Burlaga et al., 1981] in the magnetic field data immediately following the stream interaction region, again indicating that Voyager 1 was in the solar wind.

Conversely, one might imagine that event 4 has been incorrectly identified as a clean tail encounter. Although it is difficult using magnetic field data alone to unequivocally determine the exact boundaries of any distant tail event, in this case both the plasma wave and planetary radio astronomy experiments detected continuum radiation throughout this period [Lepping et al., 1983a]. Furthermore, Kurth et al. [1982] find an entry into the core of the tail during the second half of day 96 and again on days 103 and 104. Curiously, the classic magnetic signature of a tail encounter, $\lambda \approx$ 0° or 180°, does not begin until day 99 by which time the continuum radiation has become less prominent. During the first 6 days $\lambda \approx$ 90° and 270°, as expected of magnetosheath fields. A striking feature in this data is the quasi-periodic set of oscillations seen in $\underline{B}$ during days 94 - 96. These

oscillations are not present in the solar wind data as measured by Voyager 1 and are reminiscent of the 10 hour fluctuations seen in the near tail. We will explore this possibility further in the next section where the results of a spectral analysis of this interval are presented. Because of the behavior of λ, we conclude that during the first 6 or 7 days, Voyager 2 is probably not in the tail most of the time but is still in the magnetosheath. The classic signature of a tail encounter is seen only later.

Magnetic field data from the last event (5) included in this discussion are plotted in Figure 9. Again, $|\underline{B}|$ is similar in the two data sets, but the other components are quite dissimilar. At Voyager 1 λ is between 30° and 60° during most of this period, with a 1 1/2 day interlude when $\lambda \simeq 270°$. At Voyager 2 it appears that after the spacecraft spends some 3 days in the southern lobe of the tail field ($\lambda \simeq 180°$) it passes into a confused period that contains magnetosheath field ($\lambda \simeq 90°$ and 270°) and northern lobe fields ($\lambda \simeq 0°$). In the next section we will treat the two halves of this encounter separately. We turn now to an examination of the power spectra (and magnetic helicities) of these four distant tail encounter periods together with a similar analysis of the near tail fields shown in Figure 4.

4. Spectral Analysis

In addition to the many features of these near and distant tail encounters that can been inferred from the time series, power spectral analysis can supply information about periodicities and a determination of the sense and magnitude of spatial twists in these fields. The specific techniques that are used here have been described and reviewed in several places [e.g., Matthaeus and Goldstein, 1982a; Goldstein et al., 1984] and we

refer the interested reader to those sources for details. In this paper we will use only the fast Fourier transform technique to construct spectra.

We will be concerned with three spectral quantities: the trace of the power spectral matrix, denoted $S_{ii}(f)$; the spectrum of $|\underline{B}|$ which we will denote as $S_B(f)$; and the magnetic helicity spectrum, which gives a measure of the spatial handedness or twists in the field [cf. Moffatt, 1978]. As shown by Matthaeus et al. [1982] and Matthaeus and Goldstein [1982a], the magnetic helicity can be determined in homogeneous turbulence from the portion of the imaginary part of the spectral matrix that is an antisymmetric pseudotensor. The expression for the reduced magnetic helicity spectrum can then be written as

$$H_m(k_1) = 2 \text{ Im } S_{2,3}(k_1)/k_1 \tag{1}$$

Here the 1-direction is R, and the 2- and 3-directions refer to T and N, respectively. Note that $k_1 H_m(k_1)$ has the same dimensions as $S_{ii}(k_1)$. A related quantity is the normalized magnetic helicity, $\sigma_m(k_1)$, defined by

$$\sigma_m(k_1) = k_1 H_m(k_1)/S_{ii}(k_1) \tag{2}$$

This quantity is ±1 for circularly polarized transverse waves and is 0 for linearly polarized or unpolarized waves [Moffatt, 1978].

In the free flowing solar wind, data are obtained primarily along the radial direction, so that the one-dimensional spectrum $S_{ii}(k_1)$ is a reduction over the two orthogonal directions, $\hat{T}$ and $\hat{N}$ [Batchelor, 1970]. Wavenumber spectra are usually constructed from frequency spectra under the assumption of frozen-in-flow [Taylor, 1938]. However, in these data sets there are

several limitations to these spectral techniques and we will plot all spectra as a function of frequency rather than wavenumber.

The limitations arise because the Alfvén speed can be very large and the plasma convection speed small, so that frozen-in-flow is not a valid approximation. This is especially true in the near tail interval. There spectra will be treated as frequency spectra and we will not attempt a transformation into wavenumber spectra. If we assume that the signals of interest in the spectrum, among them the 10 hour rocking of the tail current sheet, originate at Jupiter and are propagating down the tail, then the sign of $H_m(f)$ reflects the spatial handedness of the twists in the magnetic field; positive values for left-handed twists and negative values for right-handed twists. Although we will generally refer to $H_m(f)$ as the magnetic helicity spectrum, it should be kept in mind that, using these techniques, a quantitative measure of the magnetic helicity can only be obtained in homogeneous MHD turbulence when frozen-in-flow is a valid assumption.

In the distant tail encounters, the Alfvén speed tends to drop and the flow speed generally increases so that one is usually in a super-Alfvénic flow regime in which the frozen-in-flow hypothesis may be assumed. Even in this situation, however, there are practical difficulties because the plasma densities are still very low ($\lesssim 10^{-2}$ cm^{-3}) and apparently highly variable. Consequently, both the plasma density and the fluid velocity are difficult to determine accurately. Without a good estimate of the mean fluid velocity, it is difficult to construct wave number spectra. A related problem is that in the distant tail encounters the relative motion of Voyager 2 often takes it across the tail into the core so that there is a large shear in the flow velocity along the spacecraft trajectory. Furthermore, the transverse speed of contractions and expansions of the tail can be of the same order as the

radial convection velocity. An additional difficulty is that when in the core of the tail, the plasma density is generally too low to estimate either the flow speed or the Alfvén speed, so that we cannot know with certainty whether or not the flow is in fact super-Alfvénic. For these reasons, only frequency spectra will be shown.

A further limitation of this analysis is that the usual assumptions about stationarity and homogeneity do not apply [Matthaeus and Goldstein, 1982b]. In the near tail interval, the rocking of the current sheet brings the spacecraft from the high latitude northern lobe of the field down into the neutral sheet and back again. Thus, we are not sampling a homogeneous plasma and only a limited amount of information can be obtained from these spectra. For example, one cannot determine the total magnetic helicity in the near tail field which in homogeneous magnetofluids is given by the integral over k_1 of equation (1) [Matthaeus et al., 1982]. Similar caveats and cautions probably apply to the distant tail spectra due to the large velocity shears across the tail. It is probably best to view these spectra as single realizations of a poorly sampled ensemble of tail encounters rather than as ensemble averages. Having said this, we will proceed with some impunity to use spectral techniques to highlight a few interesting features in these data sets.

We first consider the spectrum of the near tail interval whose time series is shown in Figure 2. The 48 s averages of the magnetic field were digitally filtered using a finite impulse response filter [Rabiner and Gold, 1975; McClellan et al., 1979] and decimated by a factor of 3. From the fast Fourier transform of the data, the spectra shown in Figure 10 were constructed. The thick line is $S_{ii}(f)$, the thin line is $S_B(f)$, and the circles and triangles are positive and negative values of $fH_m(f)$, respectively. The

spectra (power spectral density in (nT^2/Hz)) in Figure 10 have 6 degrees of freedom except that at the highest frequencies additional averaging (20 degrees of freedom) has been used for clarity.

The most prominent feature of the spectrum is the peak between 2-3 $\times$ 10^{-5} Hz. This peak corresponds to the 10 hour periodicity clearly present in the time series. (This peak is even sharper in the unsmoothed spectrum.) Nearly all of the power in this and lower frequencies is in $|\underline{B}|$. The bulge in the spectrum above a few 10^{-4} Hz arises from the significant amount of short period power evident whenever Voyager 1 approached the current sheet (cf. Figure 2). Note that the spectrum does not resemble fully developed turbulence in that the spectral shape cannot be approximated by a power law with index between -3/2 and -5/3 [Montgomery, 1983]. To some extent the shape of this spectrum is strongly influenced by all the limitations discussed above. In particular, the -5/3 power law slope predicted for fully developed turbulence is for the wave number spectrum, whereas we are only able to compute frequency spectra for this interval. Therefore, no definitive statement can be made about whether or not the fluctuations are turbulent. A curious feature of the helicity spectrum at higher frequencies is seen in Figure 10b where $\sigma_m(f)$ is plotted. Although only 6 degrees of freedom are used in these spectra, the magnitude of $\sigma_m(f)$ is small. Unlike typical solar wind spectra [Matthaeus and Goldstein, 1982a], $\sigma_m(f)$ is predominantly positive throughout much of the frequency range visible in Figure 10b . In this frequency range, much of the power may originate in the brief excursions of Voyager 2 into the neutral sheet where the field fluctuations are relatively large.

The magnetic helicity spectrum for this event suggests that the 10 hour spectral peak has a slight right-handed twist ($H_m(f) < 0$). It is possible to

estimate the pitch angle of that helical twist, denoted by α, from the value of $H_m(f)$ and we find that α is approximately given by

$$\alpha = \arcsin\sqrt{[|fH_m(f)|/S_{RR}(0)]} \qquad (3)$$

where $S_{RR}(0)$ is the power at zero frequency of the radial component of the power spectrum (alternatively, it is just the square of the mean value of the radial component, B_R). From the spectral matrix, we find that $\alpha \simeq 2°$. This value is remarkably close to the value estimated in section 2, 3°, and suggests that these small values of α may be approximately correct estimates of the twists in the field in this region of the near tail.

The distant field encounters have been analyzed in the same way except that the low pass digital filter had a narrower pass band so that the Nyquist frequency is 10^{-3} Hz. We show the Voyager 2 tail encounter spectra juxtaposed with the Voyager 1 solar wind data for comparison. The magnitude of pairs of spectra can be compared if one recalls that based on Voyager magnetic field data, Burlaga et al. [1984] found that on average, $|\underline{B}|$ varies with distance from the sun (r) as

$$|\underline{B}| \simeq 4.75\ (1 + R^2)^{1/2}/R^2 \qquad (4)$$

where R = r/AU. If we use 8.7 AU for the heliocentric distance of Voyager 2 and 10.29 AU for the distance of Voyager 1, then the Voyager 1 spectra should be increased by a factor of 1.4 for direct comparison.

The spectra for event 2 and the comparable Voyager 1 time period are shown in Figures 11a and 11b, respectively. These spectra have 26 degrees of freedom. In contrast to the near tail interval, the distant tail field of

event 2 has a power law spectrum characteristic of fully developed turbulence ($S_{ii}(f) \propto f^{-5/3}$) as does the corresponding solar wind spectrum. The frequency corresponding to a 10 hour period is marked on this and subsequent spectral plots. There is no statistically significant feature in the spectrum at that frequency.

The helicity spectrum of the tail event shows a predominance of positive values in the range 1×10^{-5} to 1×10^{-4} Hz. This suggests a tendency of the fields to twist at these rather large scales, but the relative amount of power in helical fields is generally small and is not associated with any particular spectral feature. Recall that Voyager 2 is in the northern lobe field much of the time and negative values of $H_m(f)$ might be expected for that lobe if the twists originated from the rotation of Jupiter. Thus the twists that are present are probably not a direct consequence of planetary rotation, but may reflect internal processes in the tail. The Voyager 1 solar wind data (Figure 11b) in this frequency range show no predominance of one sign of helicity over the other. A subset of this tail interval was analyzed that comprised a period when Voyager 2 was almost entirely in the northern lobe fields (this interval is noted on Figure 6a). The resulting spectrum shows evidence for a slight right-handed twist to the field (i.e., negative $H_m(f)$) at the very lowest frequencies, but does not show any significant preference for one sign of magnetic helicity above 3×10^{-5} Hz. The spectra for this subinterval are not shown.

In Figure 12a and 12b we have plotted the power spectra for event 3 and the comparable Voyager 1 time interval. These spectra also have 26 degrees of freedom and are characterized by a power law index of -5/3 over two decades. The tail event, which is another northern lobe encounter with the tail, also appears to contain left-handed twists (i.e., positive $H_m(f)$) at

the low frequencies. Again, because Voyager 2 is in the northern lobe rather than the southern lobe, these twists cannot be attributed directly to planetary rotation. The Voyager 1 solar wind interval (12b) indicates that a right-handed twist was present at the lowest frequencies associated with the high inclination of $\underline{B}$ as indicated by the large values of δ in Figure 7b. The field inclination decreased near the sector crossing; this may be the cause of the tail disconnection that Kurth et al. [1982] hypothesized occurred at about this time. Above 10^{-5} Hz both spectra have essentially randomly signed values of $H_m(f)$. The twisted fields seen in the tail event do not bear any obvious relationship to the solar wind fields as seen at Voyager 1.

We noted above that at Voyager 1 a large loop or cloud was present in the solar wind during the beginning of event 4 at Voyager 2. From the time series (Figure 8b), the decrease in λ and simultaneous increase in δ indicates that the field has left-handed spatial structure. This is reflected in Figure 13b at the lowest frequencies near 1×10^{-5} Hz where the magnetic helicity spectrum is predominantly positive. The spectrum in Figure 13a is constructed from the first 3/4 of the total time period (Figure 8a) which eliminates the large excursions of the field direction and magnitude seen at the end of the period when Voyager 2 entered the southern lobe field for about a day. The large scale (long wavelength) structures between approximately $1 - 3 \times 10^{-5}$ Hz in Figure 13b are predominantly left handed (positive helicity spectrum) as they are in the solar wind at Voyager 1. Apparently, the interplanetary loop or cloud has penetrated into the magnetosheath to the position of Voyager 2.

Of particular interest during event four are the nearly monochromatic oscillations seen in the field during days 94 through 95 (Figure 8a). No

similar oscillations are present in the corresponding Voyager 1 data. The spectrum of this short interval in shown in Figure 13c. Note the peak at 6×10^{-5} Hz corresponding to a period of 5.3 hours. The helicity in this frequency range is clearly left-handed which is not what one might expect for highly twisted northern lobe fields. However, as noted above, the identification of event 4 as a clean tail encounter is almost certainly wrong; the data in Figure 8a are probably more indicative of a mixture of tail and magnetosheath regions. The fluctuations on days 94 and 95 are probably in the magnetosheath and are reminiscent of the 5 - 10 hour magnetic fluctuations observed by Lepping et al. [1981] in the magnetosheath close to Jupiter.

Kurth et al. [1982] have discussed periodic variations in the intensity of the 1.78- and 1.0-kHz channels of the plasma wave data that also may be similar to these in event 4. One such interval occurred during some 30 hours of event 5 near day 145, which probably means that those oscillations were present when Voyager 2 was actually in the tail or, if in the magnetosheath, very close to the tail (cf. Figure 9a). No clear evidence of these fluctuations is present in the magnetic field data of the field components, but in there is a suggestion of a peak near 10 hours in the spectrum of $|\underline{B}|$ computed from the second half of event 5 (cf. Figure 14c). A second interval of periodic fluctuations, this time in the 3.11 kHz channel of the plasma wave instrument, occurred during days 42 to 54 of event 2 and was discussed by Scarf et al. [1981]. The interval that we have labelled event 2 runs from day 48 to 56. At the beginning of this time period and lasting for about one day there are periodic fluctuations present in $|\underline{B}|$ (cf. Figure 6a). The period of these oscillations is closer to 2 hours than 10 hours.

Spectra of the last tail event (5) and the Voyager 1 solar wind control

period are shown in Figure 14. We have divided event 5 (see Figure 9a) into two 4 day intervals. During the first 4 days, Voyager 2 remained in the southern lobe of the tail field. The spectrum of this data (with only 14 degrees of freedom) is shown in Figure 14a. Note that below 4×10^{-5} Hz, the magnetic helicity is positive. The solar wind field as seen at Voyager 1 also contains a predominance of positive helicity in the spectrum computed from the entire 8 day interval (cf. Figure 14b). Whether or not the positive helicity seen in the southern lobes of the tail at this distance reflects twisting of the field due to the rotation of Jupiter, as suggested by Lepping et al. [1983b], or reflects a response to external solar wind forces, or is due to some other factor, is impossible to say, but it is suggestive that this 3 day interval is a very clean one with no apparent departures of Voyager 2 from the tail.

An analysis of the second half of this event (also with 14 degrees of freedom) is shown in panel (c). During this interval Voyager 2 was moving into of the northern lobe of the tail. Note that the magnetic helicity at a few times 10^{-5} Hz is negative. It is not clear, however, that this negative helicity arises from twists in the northern lobe fields or is an artifact of the nonstationarity of the data set. If we further restrict our attention to a relatively brief interval when $\langle\lambda\rangle \simeq 0°$, enhancing the probability that we are in the northern lobe of the tail, then a different story emerges. The spectrum of this period from 0023 UT on day 145 to 1328 UT on day 146 is shown in Figure 14d. Although the spectrum has only 6 degrees of freedom, the magnetic helicity below about 7×10^{-5} Hz is now positive. Therefore, whether or not the distant tail fields contain twists arising from the rotation of Jupiter cannot be proven from these data because an unambiguous pattern of a single sign of the helicity spectrum at frequencies $\simeq 2.8 \times 10^{-5}$

Hz (i.e., periods on the order of 10 hours) is not present.

Before we continue with a discussion of these observations, it is of interest to contrast these tail events to two solar wind-like (or, more strictly, magnetosheath) time periods seen by Voyager 2. These were the periods marked A and B on Figure 4.

5. The Solar Wind Magnetic Field at Voyager 2

Intervals A and B each comprise 13 days of data. The magnetic field data and spectra from interval A are plotted in the usual formats in Figures 15a and 16a, respectively. Panels (b) of these figures contain similar data B. It is clear that at these times the solar wind magnetic fields were generally more intense than during the tail encounters. This is consistent with the fact that the tail encounters tended to occur at times of low solar wind total pressure. Intervals A and B are periods of relatively high pressure that have probably compressed the tail, moving it away from the spacecraft. During both of these intervals λ is near 90° or 270°, as expected. There appears to be at least one sector crossing during interval A. One or more sector crossings are also present in interval B.

The spectra in Figure 16 each have 26 degrees of freedom and have been digitally filtered using the same band pass filter as was used with the other time periods. The spectral index between 10^{-5} and 10^{-3} Hz is close to -5/3. There is evidence from the magnetic helicity spectrum of both time periods that large scale loops or twists are present. In general, these spectra resemble typical solar wind spectra [cf., for example, Matthaeus and Goldstein, 1982a], i.e. the relative amount of energy in helical fields is typical of solar wind data and the sign of the helicity in the inertial range

(from less than 10^{-5} to 10^{-3} Hz) is random. This is illustrated in Figure 17 where plots of $\sigma_m(f)$ are shown.

The major point of this brief digression is to show that the magnetic fields in these two intervals are typical of those often measured in the solar wind but are very different from both the tail encounter fields and the corresponding state of the solar wind as seen at Voyager 1 when corrected for solar wind convection. Recall that the time of Voyager 2 encounters with the distant tail corresponded to rarefaction flows in the solar wind (cf. Figure 5).

6. Discussion and Conclusions

We have seen that the four most prominent encounters of Voyager 2 with the distant Jovian tail supply us with a complex set of data which do not lend themselves to any single simple interpretation. For example, "event 4", when viewed in terms of the direction of the magnetic field, consists more of magnetosheath than magnetotail data and cannot be properly compared with the other events. During event 2, the time history of the magnetic field direction at the two Voyagers is very different. On the other hand, if one multiplies the spectra $S_{ii}(f)$ and $S_B(f)$ at Voyager 1 (Figures 11b) by the factor of 1.4 estimated from equation (3) to correct for the greater distance of Voyager 1, then the spectra of both the components of the field, $S_{ii}(f)$, and the magnitude of B, $S_B(f)$, are virtually identical in both absolute power level and slope above 10^{-5} Hz. [This is also approximately true of event 4 (cf. Figure 13a and 13b).] Hence although the large scale behavior of λ and δ in event 2 differ considerably from that seen at Voyager 1, the smaller scale fluctuations have the same statistical properties at the two space-

craft. This combined with the fact that $|\underline{B}|$ is roughly similar at the two spacecraft suggests that the solar wind is controlling some of the overall properties of the distant tail dynamics.

The total fluctuating power in both the magnitude and components of the field is greater at Voyager 1 during event 2 (even without renormalization) than at Voyager 2 (cf. Table 1). For event 4, the total fluctuating power in the components (without renormalization) is equal at the two Voyagers; but, the fluctuating power in the magnitude of the field is substantially greater in the solar wind at Voyager 1.

At frequencies below 10^{-4}, there is somewhat less helicity in the tail event 2 than in the corresponding Voyager 1 spectrum (cf. Figure 11), while at higher frequencies, as shown in the plots of $\sigma_m(f)$ in Figure 18, the helicity spectra are statistically indistinguishable, which in itself is rather remarkable and probably reflects the fact that the power spectrum of the field appears to have an inertial range power law of $f^{-5/3}$ as does the solar wind. The helicity spectrum can be summed over frequency to compute the total helicity with the results listed in Table 1. One should keep in mind that, because of the limitations on the validity of the spectral analysis described above, the result of that calculation cannot be thought of as a reliable estimate of the ensemble average of $\underline{A}\cdot\underline{B}$ over the volume of space sampled by the spacecraft (where $\underline{A}$ is the vector potential and $\langle\underline{A}\cdot\underline{B}\rangle$ is the definition of the magnetic helicity). Nevertheless, the results are interesting in that they show that the total helicity measured at Voyager 1 is greater, by an order of magnitude, than the helicity measured in the tail by Voyager 2.

In contrast, for event 4 which is not purely a tail event, the total helicities for the period when Voyager 2 was in the magnetosheath and tail

are essentially equal to the solar wind interval seen at Voyager 1. As with event 2, at low frequencies, between 10^{-5} and 10^{-4}, interval 4 at Voyager 2 contains significantly less helical structure than does the corresponding Voyager 1 data.

A quantitative comparison of the other two periods, 3 and 5, tells a somewhat different story. When the spectra for event 3 and the corresponding Voyager 1 interval (properly renormalized) are superimposed (cf. Figure 12), the tail event contains more total power (in both the components and field magnitude), although the shape of the spectra are similar above about 2×10^{-5} Hz. Above 10^{-4} Hz the spectrum of $|\underline{B}|$ flattens in the tail encounter data indicating that the fluctuations in this frequency range are more compressive than in the solar wind data. The relative amount of helicity in the two data sets is again comparable throughout the spectrum and especially at high frequencies as shown in the plot of $\sigma_m(f)$ (cf. Figure 12 and 19). The total helicity (Table 1) is also approximately the same in the two data sets except that the sense of handedness is opposite. This is also the event that Kurth et al. [1982] concluded had disconnected from Jupiter about midway through its duration.

Event 5 is difficult to characterize in this context because we had to divide the tail encounter period into two parts to preserve a single lobe character in each analysis. When compared to the Voyager 2 interval (Figure 14a and c), the solar wind period observed at Voyager 1 has more power than is contained in either half of event 5 (Table 1). This is even more true if event 5 is considered as a whole, though we have not plotted those spectra. The total helicity for event 5 is rather small, which is a reflection of the fact that the first 4 days and second 4 days have opposite total helicities. The corresponding solar wind interval at Voyager 1 has considerably more

helical power than does the tail event.

Perhaps in these distant tail encounters, we are seeing an evolution from the non-turbulent, slightly helical fields of the near tail (Figure 10), to more turbulent ($f^{-5/3}$ spectrum), but relatively non-helical fields of the distant tail. Whether the $f^{-5/3}$ spectrum seen in the distant tail events reflects leakage of fluctuations into the tail from the solar wind-like magnetosheath, or is the result of dynamical processes within the tail itself remains unclear, although the relative orderliness of the large scale tail fields, most obvious in λ, suggests that at least some of the fluctuations arise from internal processes.

7. Summary

In the near tail the 10 hour rotation of Jupiter is clearly evident in the power spectrum. The fields have relatively little helicity, but the sense and magnitude of the twist (a pitch angle of approximately 2° - 3°) in the magnetic field in this region of the spectrum are consistent with the right hand orientation expected in the northern lobe of the tail, where the measurements were made, assuming that the twist is due to the field being anchored to a spinning planet. This estimate of the pitch angle was made using two different techniques and using different plasma parameters. In addition, the power spectrum of both the components and magnitude of the field are not well described by a single power law index and it does not appear that the near tail of Jupiter is turbulent.

Whether the twisting of the field by the rotation of Jupiter persists into the distant tail cannot be ascertained with certainty. The cleanest distant tail encounter, in the sense that the spacecraft remained entirely in

one lobe for a significant period of time, is the first half of event 5. Voyager 2 was in the southern lobe of the distant tail and there the helicity at the lowest frequencies is clearly positive (left hand) as expected. The second half of this interval is a complex one in which Voyager 2 is apparently moving in and out of the northern lobe. When analyzed as a whole, the helicity at the lowest frequencies is in fact negative; but when the analysis is confined to the relatively short time interval during which the radial fields are positive definite, i.e. brief excursions into the southern lobe are excluded, then the helicity at low frequencies becomes positive.

From this limited amount of data it is therefore difficult to prove or disprove the hypothesis offered by Lepping et al. [1983b] that twisting of the tail fields due to the rotation of Jupiter will build up to the point that a significant centrifugal pressure is created that will help support the tail against collapse. This analysis also suggests that application of a simple Faraday disk dynamo model to solar wind interactions with planetary magnetospheres [see, for example, Hill et al., 1983] may need modification to include the effects of shears in the helical fields that could be generated across a broad region of the magnetotail if significant velocity gradients existed across the tail between the magnetosheath and the tail axis. We see evidence in this investigation that helical structures are not an omnipresent feature of the distant Jovian tail.

A low frequency oscillation in the components and magnitude of $\underline{B}$ also appears during event 4, and perhaps at the beginning of event 2. During event 4 the period is close to 5.3 hours in the spacecraft frame of reference and the sense of helical twist was left-handed. These fluctuations are apparently propagating in the magnetosheath and not in the tail itself. They may be related to the oscillations present in the plasma wave data reported

by Kurth et al. [1982] and Scarf et al. [1981] as well as to the 5 - 10 hour magnetic field variations near Jupiter described by Lepping et al. [1981]. During the second half of event 5, when Voyager 2 was either very close to the tail but still in the magnetosheath, or had just entered the northern lobe of the tail, there is a suggestion of a 10 hour peak in the spectrum of $|\underline{B}|$. The magnetic field in this region of the spectrum has essentially zero helicity, so whatever the origin of this fluctuation in $|\underline{B}|$, it is unlikely that it is directly related to twisting of the magnetic field due to planetary rotation.

A general property of the distant tail encounters, which one should recall were originally identified by the presence of continuum radiation and low densities, with later consideration of the magnetic field data in a supporting role, is that the large scale magnetic field within the tail is generally well-ordered. The longitude of the field λ in the distant tail tends to be either close to 0° or 180°. It was this property of the distant encounters that led us to conclude that much of "event 4" was, in fact, magnetosheath and not purely a tail region.

We have confirmed that encounters with the distant tail are clearly associated with solar wind stream rarefaction regions by using Voyager 1 magnetic field data as a monitor of solar wind conditions during these four prominent tail events. As Voyager 2 penetrates more deeply into the tail, $|\underline{B}|$ usually decreases even further from its already low magnetosheath value.

The Voyager 1 data has also provided evidence that during event 2 there was no sector crossing in the solar wind. As a consequence, the similar time history of the magnetic field noticed by Lepping et al. [1982] as Voyager 2 first approached and then receded from the core of the tail probably represents a time symmetric motion of the tail past the spacecraft rather

than the motion of Voyager 2 through a warped current sheet. Picturing all of the prominent tail encounters as the result of time symmetric motion is also consistent with the view put forth by Lepping et al. [1983] that the Jovian tail has a sausage-string shape to a first approximation.

Similarly, we found that an interplanetary sector crossing did occur during event 3 as predicted by Kurth et al. [1982] based on the disappearance of continuum radiation during the tail encounter. The existence of a sector crossing could have initiated magnetic reconnection that would erode the tail and cause it to disconnect from Jupiter as argued by Kurth et al.

From a comparison of the power spectra of the tail, magnetosheath and solar wind data sets we have found that at frequencies of a few 10^{-5} Hz, the helicity spectra of the distant tail and solar wind tend to differ. During events 2, 3 and the first 4 days of event 5 there are large scale twists in the tail fields that are not generally present in the corresponding solar wind data at Voyager 1. The sense of these twists in events 2 and 3 is inconsistent with their originating in planetary rotation and must therefore derive from processes internal to the tail dynamics itself or from the solar wind interaction with the tail.

At higher frequencies, 10^{-4} to 10^{-3} Hz, we found that the distant tail spectra are indistinguishable from solar wind spectra in shape. That is, the distant tail spectra are characterized by a single power law over several decades and the power law index is -5/3. Furthermore, the helicity spectra in this frequency range are statistically identical in the sense that in all data sets the sign and magnitude of the normalized helicity, $\sigma_m(f)$, tend to be equal. Thus, at frequencies between 10^{-4} and 10^{-3} Hz, the fluctuating fields in the distant tail appear to be turbulent with a Kolmogoroff type of spectrum. This turbulence may reflect simple leakage or diffusion of solar

wind fields into the tail, or may be a consequence of dynamical processes occurring within the tail itself. The limited amount of data available precludes definitive answers to that question.

Acknowledgments: We express our appreciation to L. F. Burlaga for his many stimulating comments during the course of this research and for his critical reading of early versions of this manuscript. In addition, we thank N. F. Ness and H. S. Bridge, principal investigators of the Voyager magnetic field and plasma experiments, respectively, for their support. M. Harrison is particularly thanked for her assistance in preparing the data tapes for this analysis. Stimulating discussions with K. Schatten and W. H. Matthaeus are also acknowledged.

References

Batchelor, G. K., Theory of Homogeneous Turbulence, Cambridge Univ. Press 1970.

Behannon, K. W., L. F. Burlaga, and N. F. Ness, The Jovian magnetotail and its current sheet, J. Geophys. Res., 86, 8385, 1981.

Burlaga, L. F., K. W. Klein, R. P. Lepping, and K. W. Behannon, Large-scale interplanetary magnetic fields: Voyager 1 and 2 observations between 1 AU and 9.5 AU, J. Geophys. Res., in press, 1984.

Burlaga, L. F., E. Sittler, F. Mariani, and R. Schwenn, Magnetic loop behind an interplanetary shock: Voyager, Helios, and IMP 8 observations, J. Geophys. Res., 86, 6673, 1981.

Dessler, A. J., and R. D. Juday, Configuration of auroral radiation in space, Planet. Space Sci., 13, 63, 1965.

Goldstein, M. L., L. F. Burlaga, and W. H. Matthaeus, Power spectral signatures of interplanetary corotating and transient flows, J. Geophys. Res., 89, 3747, 1984.

Grzedzielski, S., W. Macek, and P. Oberc, Expected immersion of Saturn's magnetosphere in the Jovian magnetic tail, Nature, 292, 615, 1981.

Gurnett, D. A., W. S. Kurth, and F. L. Scarf, The structure of the Jovian magnetotail from plasma wave observations, Geophys. Res. Lett., 7, 53, 1980.

Hill, T. W., A. J. Dessler, and M. E. Rassbach, Aurora on Uranus: A Faraday disk dynamo mechanism, Planet. Space Sci., 31, 1187, 1983.

Kurth, W. S., D. A. Gurnett, F. L. Scarf, and R. L. Poynter, J. D. Sullivan, Voyager observations of Jupiter's distant magnetotail, J. Geophys. Res., 86, 8402, 1981.

Kurth, W. S., J. D. Sullivan, D. A. Gurnett, F. L. Scarf, H. S. Bridge, and E.

C. Sittler, Observations of Jupiter's distant magnetotail and wake, J. Geophys. Res., 87, 10373, 1982.

Lepping, R. P., L. F. Burlaga, L. W. Klein, J. M. Jessen, and C. C. Goodrich, Observations of the magnetic field and plasma flow in Jupiter's magnetosheath, J. Geophys. Res., 86, 8148, 1981.

Lepping, R. P., L. F. Burlaga, M. D. Desch, and L. W. Klein, Evidence for a distant (> 8700 R_J) Jovian magnetotail, Geophys. Res. Lett., 9, 885, 1982.

Lepping, R. P., M. D. Desch, L. W. Klein, E. C. Sittler, Jr., J. D. Sullivan, W. S. Kurth, and K. W. Behannon, Structure and other properties of Jupiter's distant magnetotail, J. Geophys. Res., 88, 8801, 1983a.

Lepping, R. P., K. H. Schatten, and E. C. Sittler, Magnetic field inhibition of plasma entry into the distant Jovian magnetotail, EOS, 64, 795, 1983b.

Matthaeus, W. H., M. L. Goldstein, and C. W. Smith, Evaluation of magnetic helicity in homogeneous turbulence, Phys. Rev. Lett., 48, 1256, 1982.

Matthaeus, W. H., and M. L. Goldstein, Measurements of the rugged invariants of magnetohydrodynamic turbulence in the solar wind, J. Geophys. Res., 87, 6011, 1982a.

Matthaeus, W. H., and M. L. Goldstein, Stationarity of magnetohydrodynamic fluctuations in the solar wind, J. Geophys. Res., 87, 10347, 1982b.

McClellan, J. H., T. W. Parks, and L. R. Rabiner, FIR linear phase filter design program, in Program for Digital Signal Processing, Digital Signal Processing Committee, editor, IEEE Press, 1979.

Moffatt, H. K., Magnetic Field Generation In Electrically Conducting Fluids, Cambridge University Press, 1978.

Montgomery, D. C., Theory of hydromagnetic turbulence, in Solar Wind Five, M. Neugebauer, editor, NASA Conference Publication 2280, 1983.

Ness, N. F., M. H. Acuña, R. P. Lepping, L. F. Burlaga, K. W. Behannon, and F.

M. Neubauer, Magnetic field studies at Jupiter by Voyager 1: Preliminary results, Science, 204, 982, 1979a.

Ness, N. F., M. H. Acuña, R. P. Lepping, K. W. Behannon, L. F. Burlaga, and F. M. Neubauer, Jupiter's magnetic field, Nature, 280, 799, 1979b.

Ness, N. F., M. H. Acuña, R. P. Lepping, L. F. Burlaga, K. W. Behannon, and F. M. Neubauer, Magnetic field studies at Jupiter by Voyager 2: Preliminary results, Science, 206, 966, 1979c.

Rabiner, L. R., and B. Gold, Theory and Application of Digital Signal Processing, Prentice-Hall Inc., Englewood Cliffs, New Jersey, 1975.

Scarf, F. L., Possible traversals of Jupiter's distant magnetic tail by Voyager and Saturn, J. Geophys. Res., 84, 4422, 1979.

Scarf, F. L., W. S. Kurth, D. A. Gurnett, H. S. Bridge, and J. D. Sullivan, Jupiter tail phenomena upstream from Saturn, Nature, 292, 585, 1981.

Siscoe, G. L., Two magnetic tail models for Uranus, Planet. Space Sci., 19, 483, 1971.

Taylor, G. I., The spectrum of turbulence, Proc. Roy. Soc. A, 164, 476, 1938.

TABLE 1. Summary of Properties of Data Sets Analyzed

Interval (V2 = Voyager 2) (V1 = Voyager 1)	Fluctuating Energy $\sum_f S_{ii}(f)$ (nT^2)	Fluctuating Energy $\sum_f S_B(f)$ (nT^2)	Degrees of Freedom	Helicity $\sum_f H_m(f)$ (nT^2/Hz)
V2 Tail Event 2	0.024	0.0054	26	-13.2
V1 Solar Wind Control 2	0.030	0.0109	26	-199.1
V2 Tail Event 3	0.072	0.0087	26	1240.0
V1 Solar Wind Control 3	0.044	0.0023	26	-1034.9
V2 Tail Event 4	0.064	0.0050	26	2052.0
V1 Solar Wind Control 4	0.064	0.0129	26	2581.4
Subset of Tail Event 4 Day 94 0923:47 to Day 96 0916:35	0.009	0.0030	10	25.08
V2 Tail Event 5	0.038	0.0107	26	7.36
V1 Solar Wind Control 5	0.060	0.0137	26	-711.6
First 4 days of Tail Event 5:	0.026	0.0128	14	60.4
Second 4 days of Tail Event 5:	0.018	0.0035	14	-108.0
Subset of second 4 days of Tail Event 5 (Day 145 0023 to Day 146 1328)	0.011	0.0019	6	5.0
Near tail (V1)	2.112	1.64	6	-2828.0
V2:				
Magnetosheath Control A	0.228	0.0343	26	2511.6
Magnetosheath Control B	0.199	0.0219	26	603.3

Figure Captions

Figure 1. The Jupiter encounter trajectory of Voyager 1 in planetocentric orbital coordinates (the x-y plane is the orbital plane, +x is toward the sun and +z is northward), in units of Jupiter radii (R_J = 71 398 km). The day of year (1979) is labeled on the trajectory. Model magnetopause and bow shock curves are from Lepping et al. [1981]. The cross-hatched area is the 3 1/2 day region in the near-tail of interest. The figure is adapted from Behannon et al. [1981].

Figure 2. The magnetic field (in nT) measured by Voyager 1 between 80 and 139 R_J downstream from Jupiter in the Jovian tail. The data are from 48 s averages that have been further digitally filtered to a resolution of 144 s. The heliographic spherical coordinates (λ, δ and $|\underline{B}|$, see text) of $\underline{B}$ are plotted. Note that the spacecraft is in the northern lobe field during this time ($\lambda \simeq 30°$).

Figure 3. The Voyager 2 trajectory in cylindrical coordinates (top) and in Jupiter orbital plane coordinates (bottom) in units of Jupiter radii. The X′ axis is also in Jupiter's orbital plane, but aberrated by 1.8° from X to account for the tail's angular displacement by Jupiter's motion in a 420 km/s solar wind. Tail encounter events K,K,1,...,8, are those discussed by Lepping et al. [1983]. The distance $\rho'_{C.A.}$ refers to the closest approach distance between Voyager 2 and the X′ axis. Only the most prominent tail encounter events (2,3,4,5) are discussed here.

Figure 4. An overview of two-hour average magnetic field data (in nT) covering the time period from day 30 to day 160 (1981) when Voyager 2 is between 6000 and 7500 R_J from Jupiter. At the top of the figure, two solar wind control intervals, denoted A and B, and tail encounter intervals 2 - 5 are indicated. The tic marks on the time axis are spaced 5 days apart.

Figure 5. A plot similar to Figure 4 showing the solar wind magnetic field as measured at Voyager 1. The general field patterns seen in Figure 4 are repeated here with a delay of approximately 5 1/2 days.

Figure 6. (a) (Top) Event 2 as recorded by Voyager 2. The time axis covers 8 days (the tic marks are spaced every 24 hours) from day 48 to day 56 (1981). In the top two panels 13 minute averages of the ion density and speed are shown. The cross-hatched regions are taken from Table 2 of Kurth et al. [1982] and are based on their estimates of PLS densities to be lower than about 10^{-2} cm^{-3}. The speed is plotted only outside of the cross-hatched regions, since it is not well determined for times when the density is $< 10^{-2}$ cm^{-3}. In the remaining panels, 8 minute averages of the magnetic field are plotted in heliographic spherical coordinates. The regions denoted as cores in the magnetic field magnitude panel are based on abrupt intensifications and drops in the low-frequency cutoff of the plasma continuum radiation listed in Table 1 of Kurth et al. [1982]. (b) (Bottom) Eight days of solar wind magnetic field data as recorded by Voyager 1 from day 54 to day 62. The 5 1/2 day shift in the data allows for the convection of the solar wind from the position of Voyager 2 to Voyager 1 which was 1.6 AU downstream.

Figure 7. (a) (Top) Similar to Fig. 6, but for event 3. The time axis covers 13 days from day 66 to day 79. (b) (Bottom) The same period as seen at Voyager 1. Only 9 days of data are shown because during the first few days of this period Voyager 1 was still in the compression region of the preceding stream interaction.

Figure 8. (a) (Top) Similar to Fig. 6, but for event 4. The time axis covers 12 days from day 92 to day 104. Note the quasi-periodic oscillations during days 94 and 95. (b) (Bottom) The same period as seen at Voyager 1 from days 96 to 108.

Figure 9. (a) (Top) Event 5 as seen by Voyager 2. Nine days of data are displayed from day 140 to day 149. Early in the event the spacecraft is in the southern lobe and passes into the northern lobe midway through the event. Occasional penetrations back into the southern lobe occur throughout the second half. (b) (Bottom) The same period recorded at Voyager 1 from days 146 to 155.

Figure 10. (a) Power spectra in nT^2/Hz for the near tail encounter (cf. Figure 2). Plotted as the thick line is $S_{ii}(f)$. The thin line is $S_B(f)$ and $fH_m(f)$ is shown as circles (positive values) and triangles (negative values). The 48 s average magnetic field data have been digitally filtered and decimated using a low pass filter so that the Nyquist frequency is at 3×10^{-3} Hz. Note the strong spectral peak between 2 and 3×10^{-5} Hz which reflects the 10 hour period of the rocking of the current sheet. In this spectral band the magnetic helicity is predominantly negative as expected if the magnetic fields are being wound into a right-handed helix by the rotation of Jupiter. The error bar on this and subsequent figures represents a 90% confidence level. Refer to the text for further details. (b) The normalized magnetic helicity $\sigma_m(f)$ plotted on a linear scale to emphasizes the relative lack of helical structure in these fields at higher frequencies.

Figure 11. (a) Power spectra in nT^2/Hz for event 2. The time series is shown in Figure 6a. The quantities plotted are the same as in Figure 1, except that here and in the following figures the 48 s average magnetic field data from Voyager 2 have been digitally filtered and decimated using a low pass filter with a lower high frequency cutoff which places the Nyquist frequency at 10^{-3} Hz. This spectrum (and all the following ones) have a power law slope of $f^{-5/3}$ which may be characteristic of fully developed turbulence. (b) Power spectra computed from the Voyager 1 interval shown in Figure 6b.

Figure 12. (a) Similar to Figure 11 except for event 3. The time series is from Figure 7a. (b) Power spectra computed from the Voyager 1 interval shown in Figure 7b.

Figure 13. (a) Similar to Figure 11 except for event 4. The time series is from the first 3/4 of Figure 8a (days 92 - 98). (b) Power spectra computed from the Voyager 1 interval shown in Figure 8b. See the text for a discussion of the two helicity spectra. (c) Voyager 2 power spectra of the short interval covering days 94 and 95 from Figure 8a. Note the spectral peak at 5.3 hour period.

Figure 14. (a) Similar to Figure 11 except for the first half of event 5 shown in Figure 9a. (b) Power spectra computed from the Voyager 1 interval shown in Figure 9b. (c) Power spectra for the second half of event 5 shown in Figure 9a. (d) Power spectra of the short interval of Voyager 2 northern lobe data discussed in the text.

Figure 15. (a) Magnetic field data from control interval A (cf. Figure 4). The plot spans 13 days from day 29 to day 42 (1981). (b) Magnetic field data from control interval B (cf. Figure 4). The plot spans 13 days from day 120 to day 133 (1981).

Figure 16. (a) Power spectrum of the Voyager 2 control interval A in Figure 15a. (b) Power spectrum of the Voyager 2 control interval B in Figure 15b.

Figure 17. Plots of $\sigma_m(f)$ for the control intervals whose spectra appear in Figure 16.

Figure 18. (a) (Bottom) Plots of $\sigma_m(f)$ for tail event 2 and (b) (Top) the corresponding solar wind control. The power spectra are shown in Figure 11.

Figure 19. (a) (Bottom) Plots of $\sigma_m(f)$ for tail event 3 and (b) (Top) the corresponding solar wind control. The power spectra are shown in Figure 12.

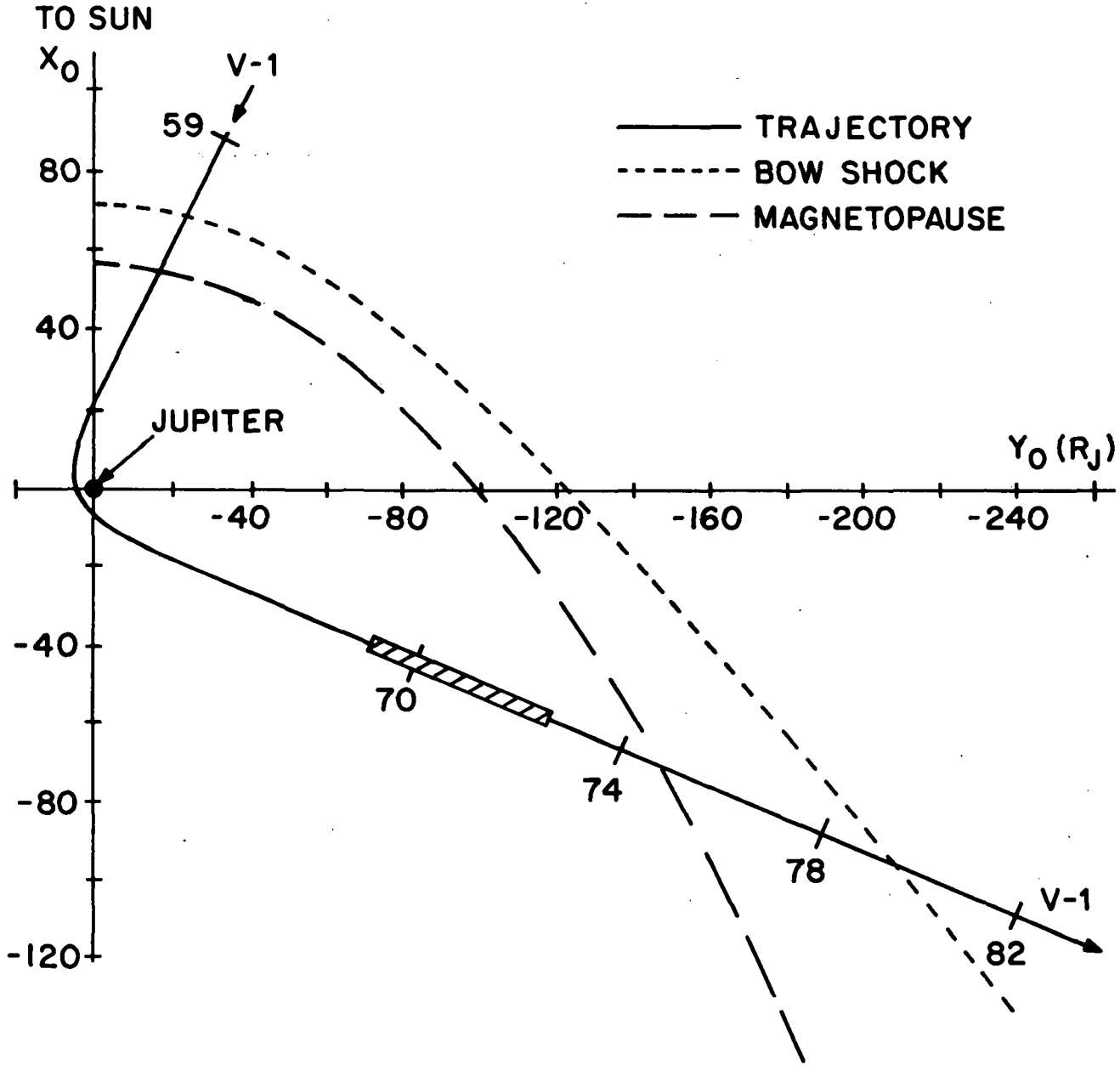
TO SUN
X_0
V-1
59
80
40
-40
-80
-120
JUPITER
Y_0 (R_J)
-40
-80
-120
-160
-200
-240
70
74
78
82
V-1
TRAJECTORY
BOW SHOCK
MAGNETOPAUSE

Figure 1

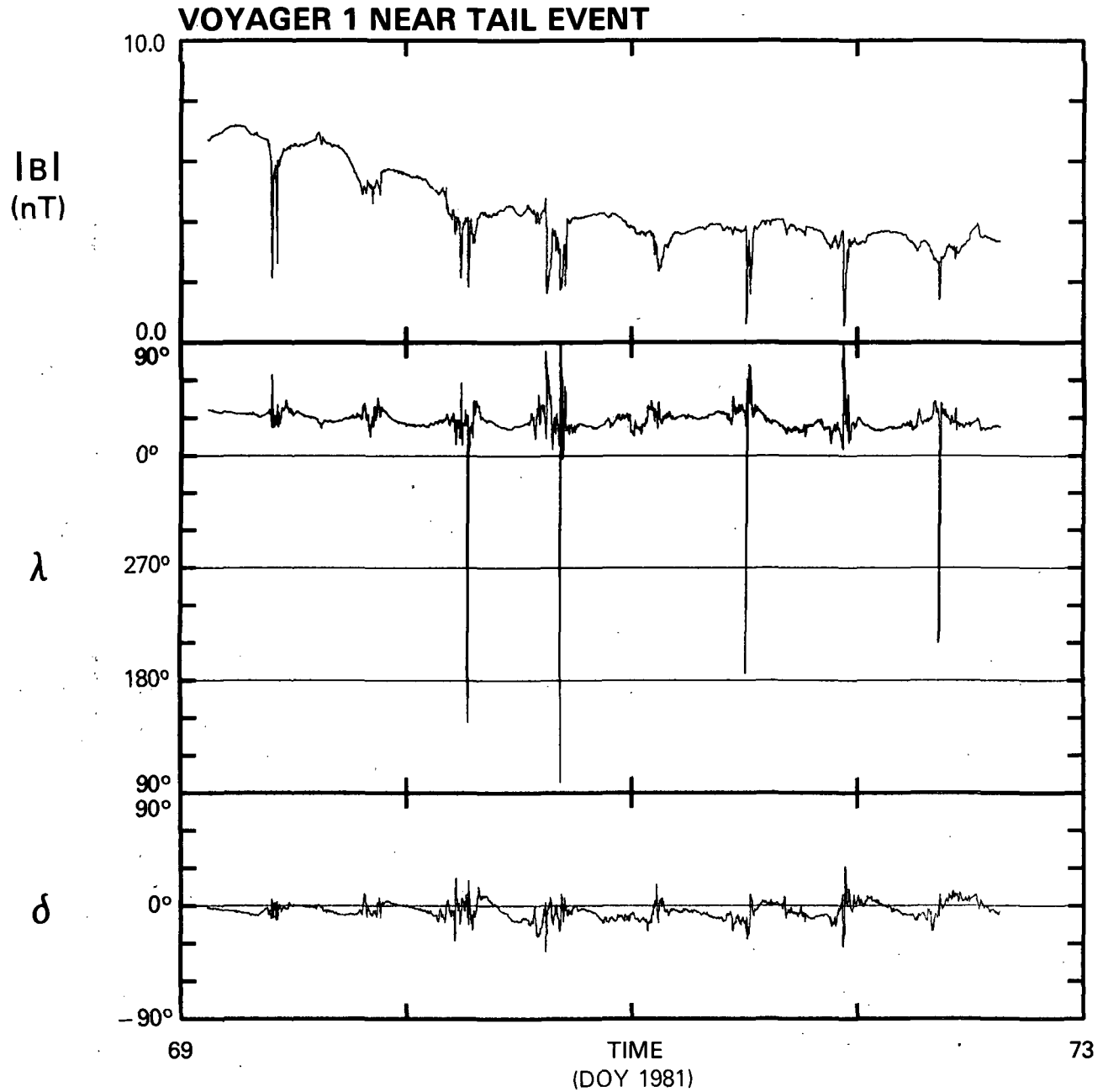
VOYAGER 1 NEAR TAIL EVENT
10.0
|B|
(nT)
0.0
90°
0°
λ
270°
180°
90°
90°
δ
0°
−90°
69
TIME
(DOY 1981)
73

Figure 2

VOYAGER 2 TRAJECTORY

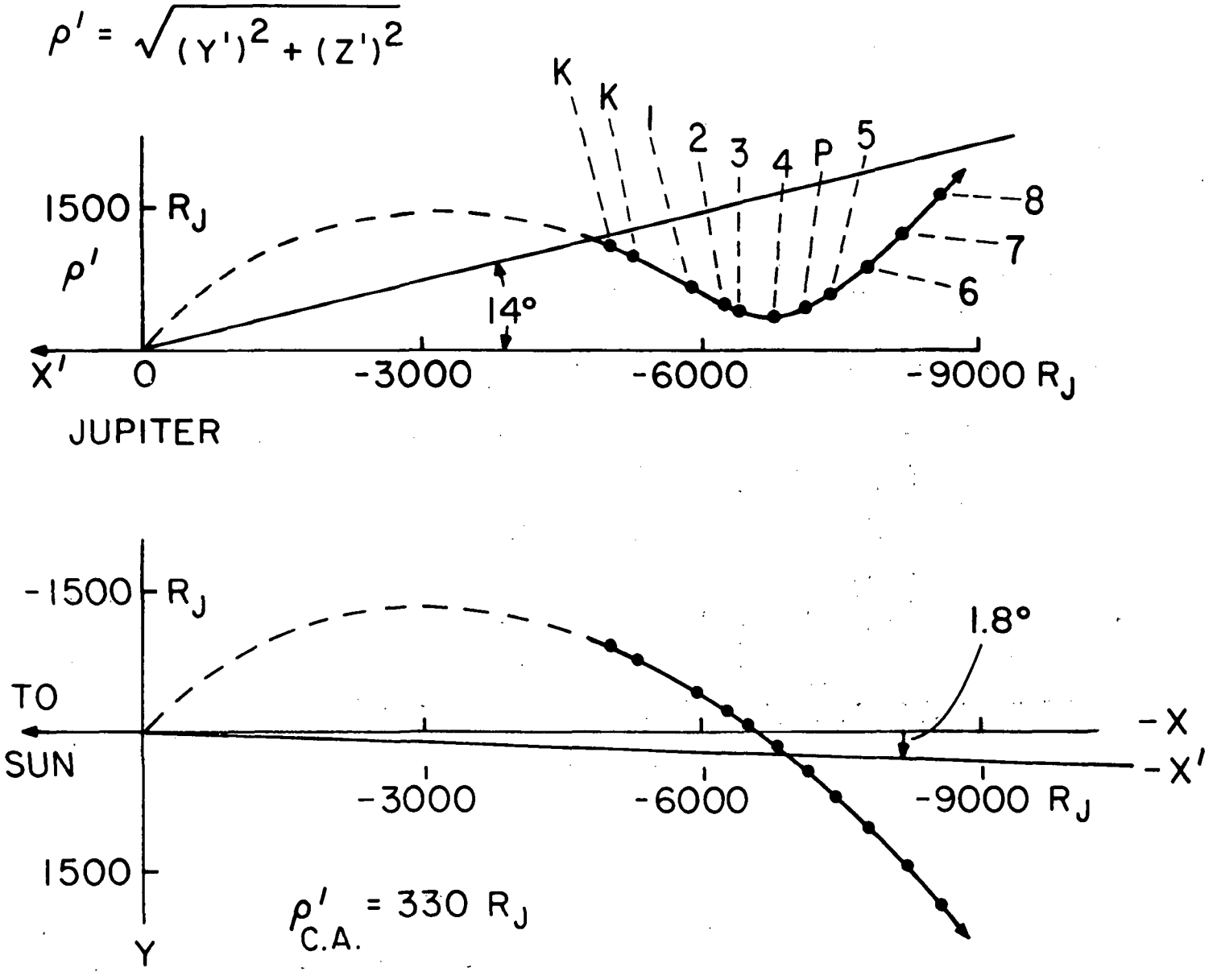

Figure 3

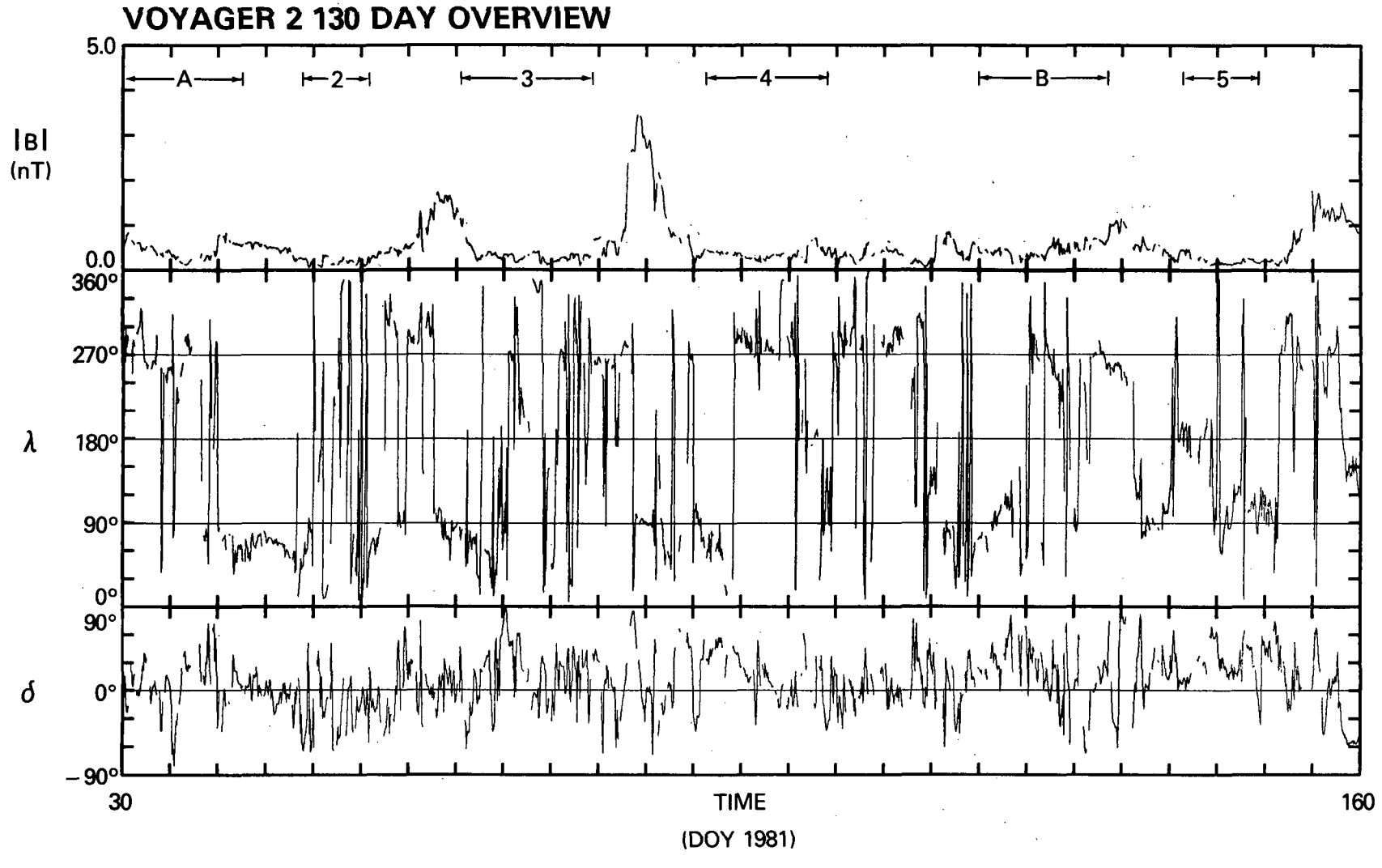
VOYAGER 2 130 DAY OVERVIEW
5.0
A
2
3
4
B
5
|B|
(nT)
0.0
360°
270°
λ
180°
90°
0°
90°
δ
0°
−90°
30
TIME
160
(DOY 1981)

Figure 4

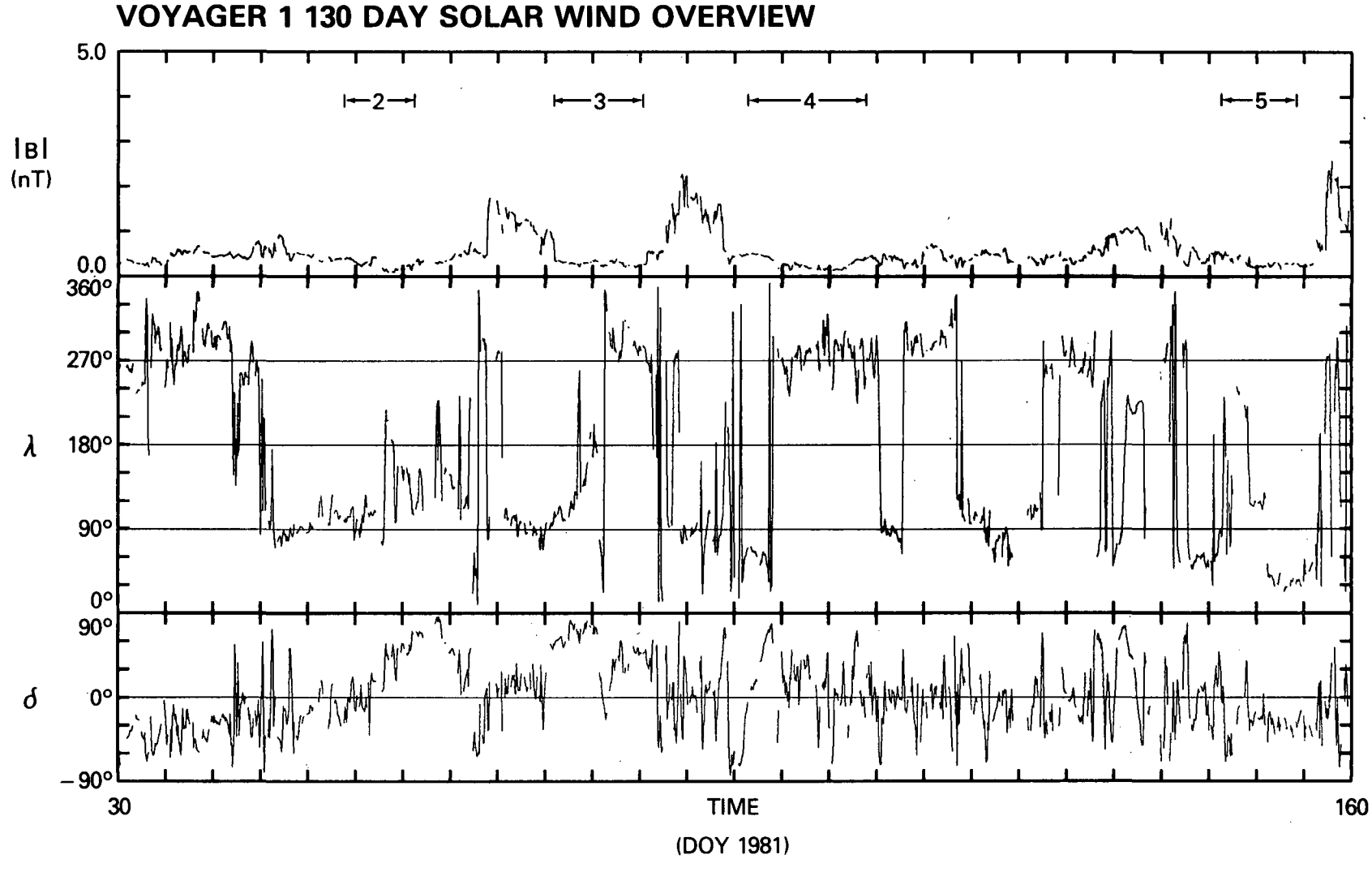
VOYAGER 1 130 DAY SOLAR WIND OVERVIEW
5.0
|B|
(nT)
0.0
2
3
4
5
360°
270°
λ
180°
90°
0°
90°
δ
0°
−90°
30
TIME
160
(DOY 1981)

Figure 5

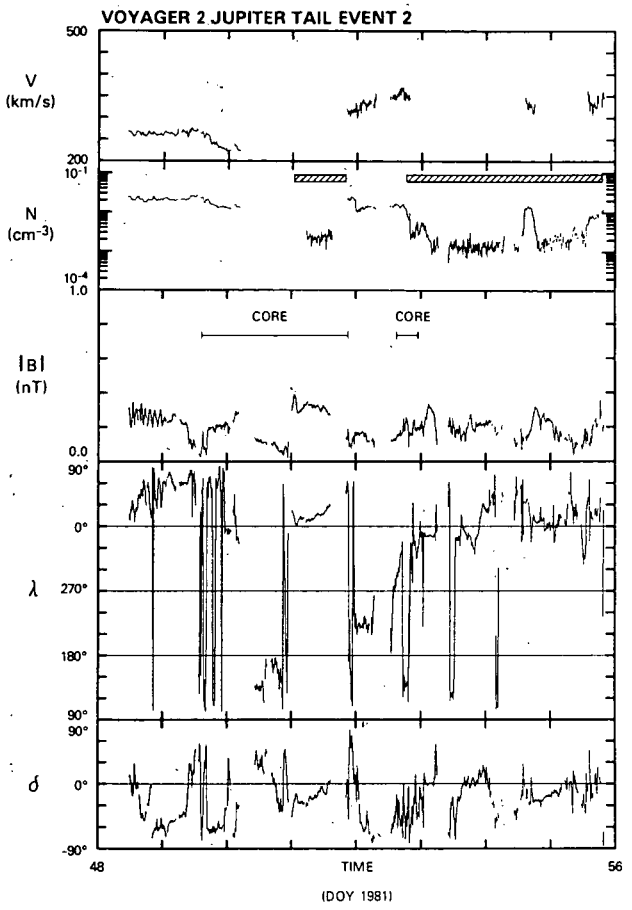

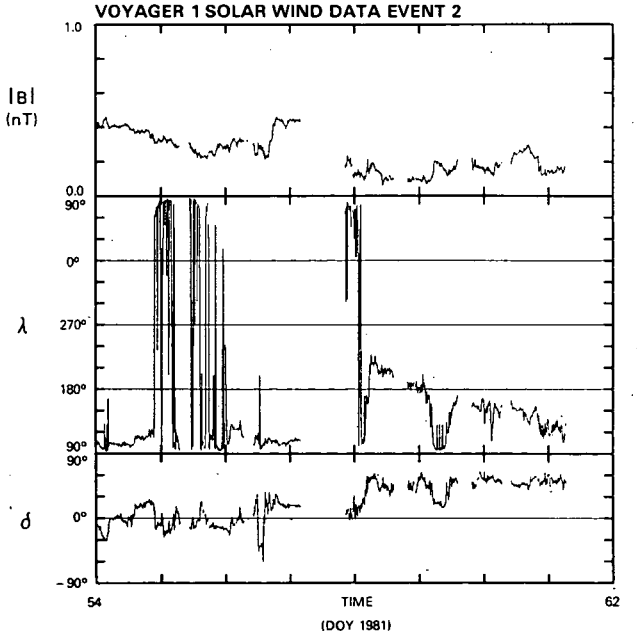

Figure 6

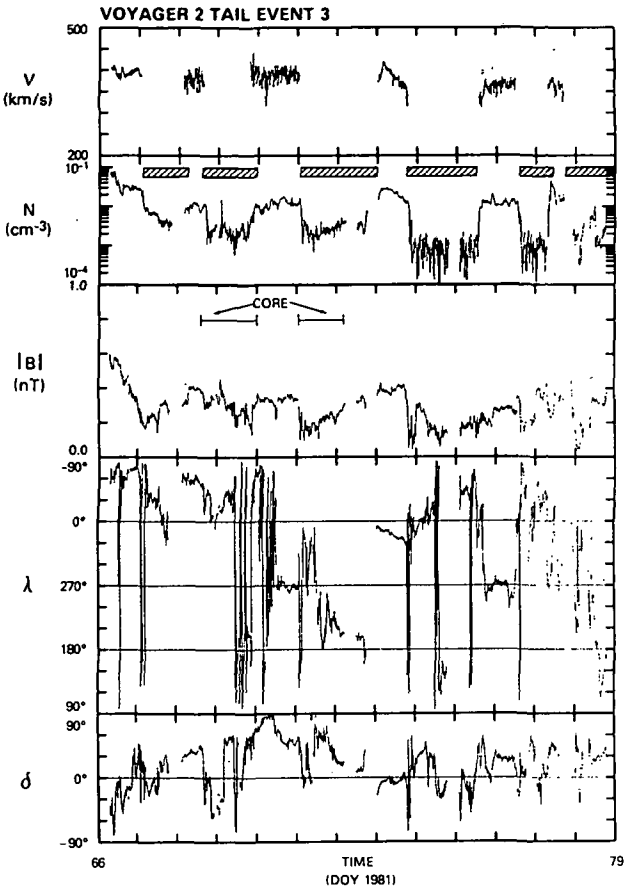

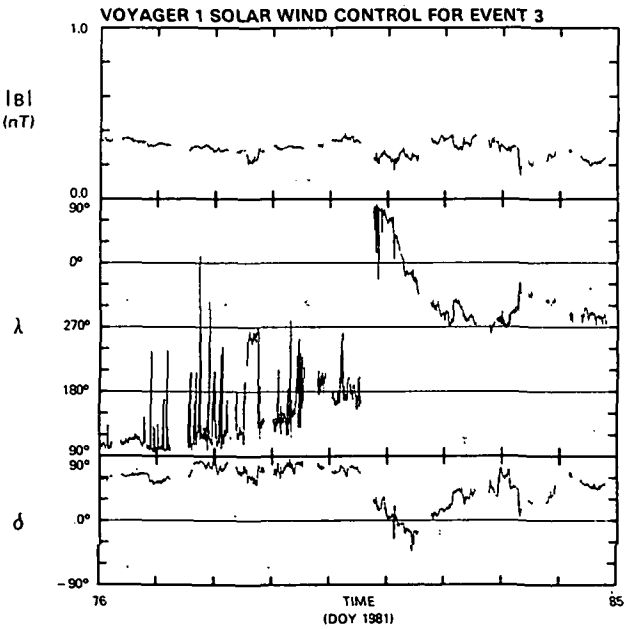

Figure 7

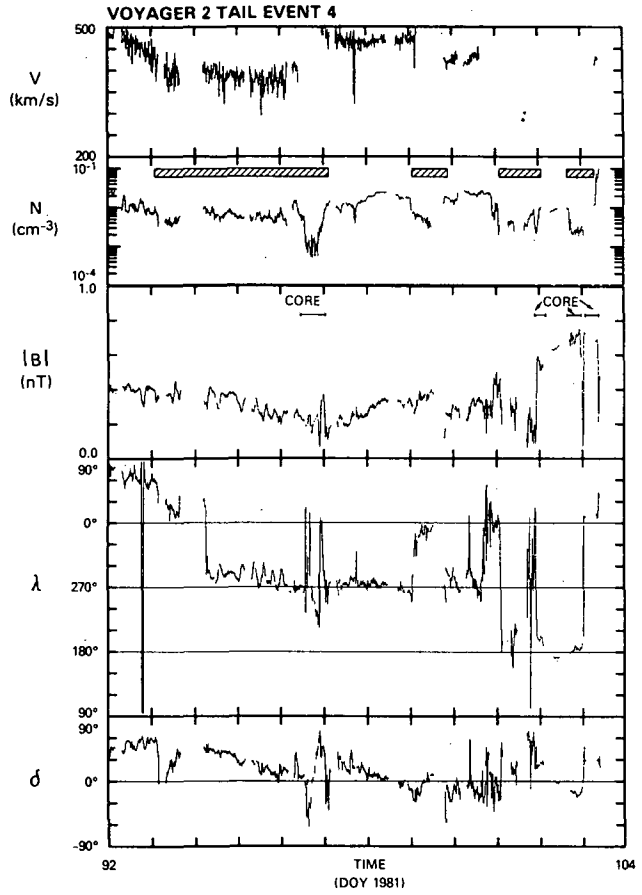
VOYAGER 2 TAIL EVENT 4
V
(km/s)
500
200
N
(cm-3)
10-1
10-4
CORE
CORE
|B|
(nT)
1.0
0.0
λ
90°
0°
270°
180°
90°
δ
90°
0°
-90°
92
TIME
(DOY 1981)
104

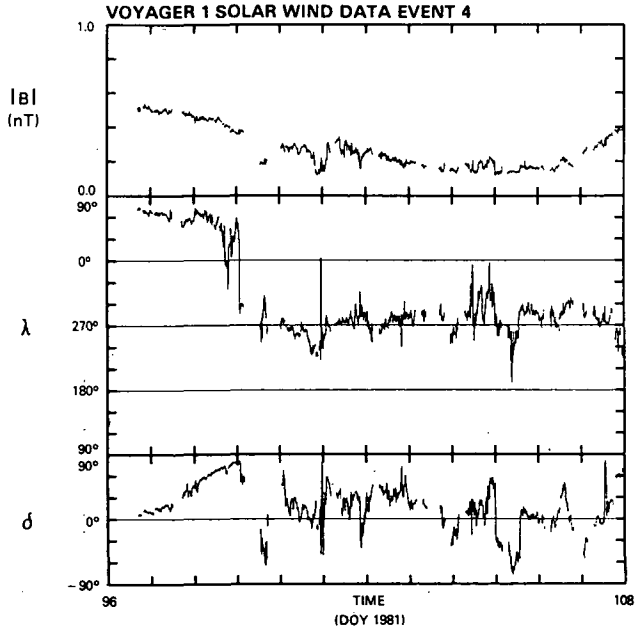
VOYAGER 1 SOLAR WIND DATA EVENT 4
|B|
(nT)
1.0
0.0
λ
90°
0°
270°
180°
90°
δ
90°
0°
-90°
96
TIME
(DOY 1981)
108

Figure 8

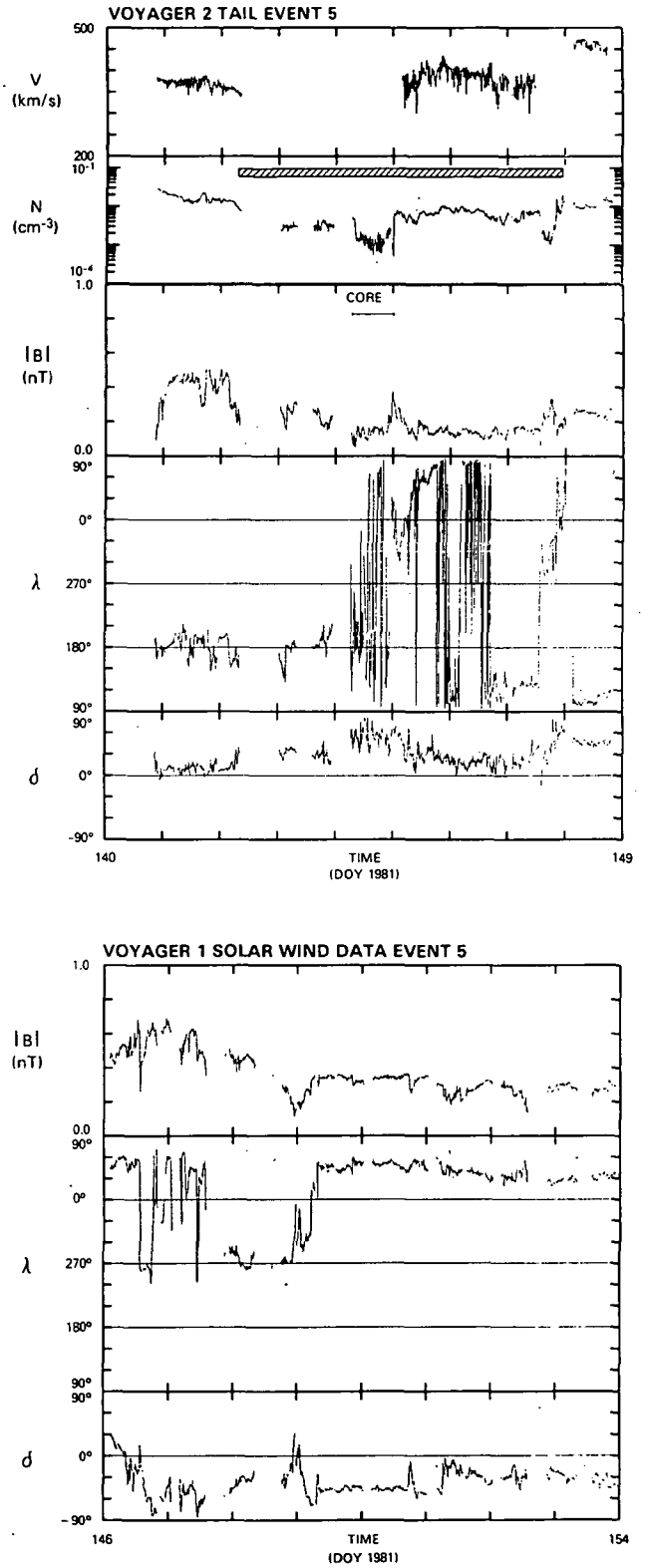

Figure 9

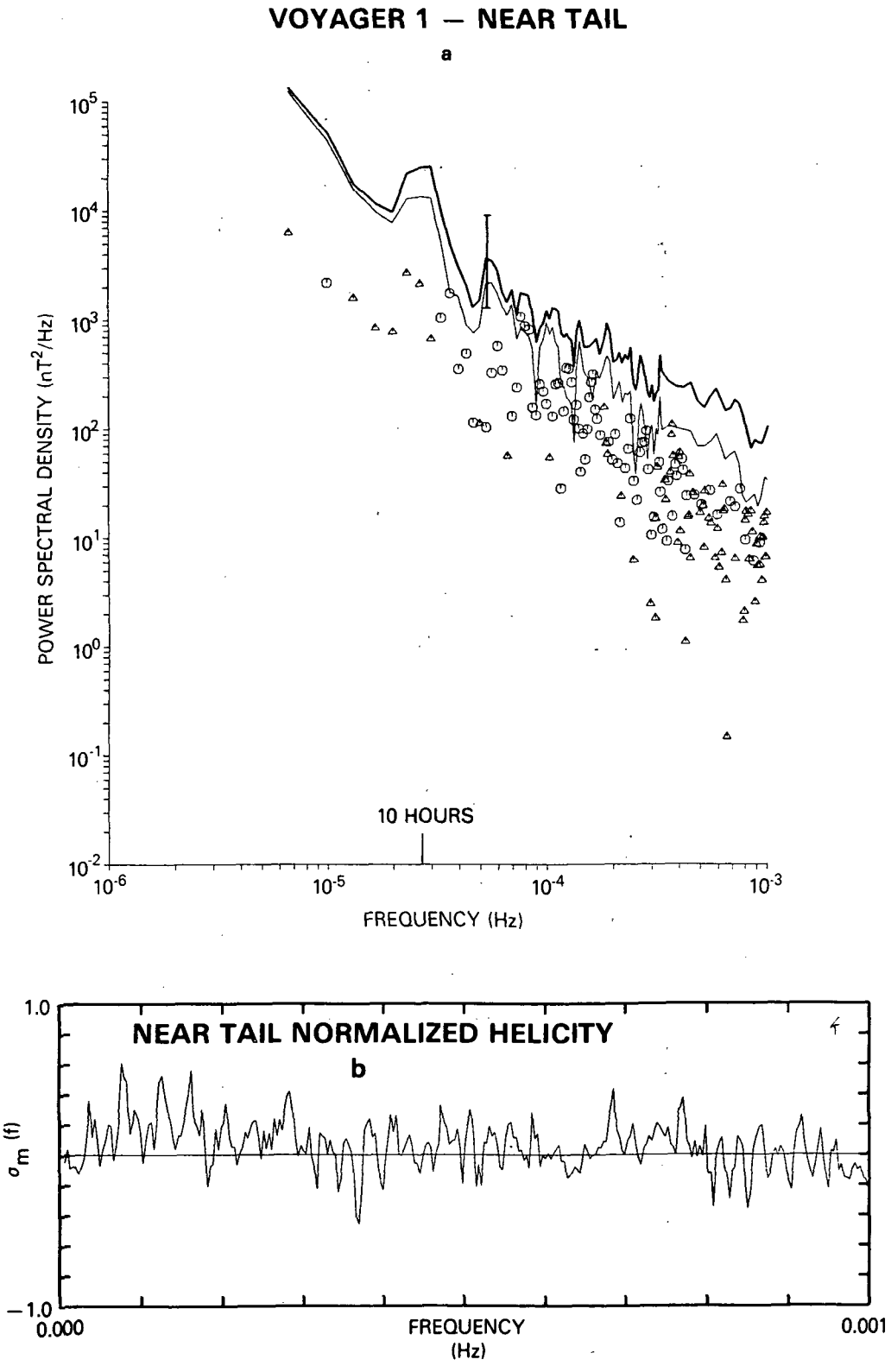
VOYAGER 1 — NEAR TAIL
a
POWER SPECTRAL DENSITY (nT²/Hz)
10 HOURS
FREQUENCY (Hz)
NEAR TAIL NORMALIZED HELICITY
b
σm (f)
1.0
−1.0
0.000
FREQUENCY
(Hz)
0.001

Figure 10

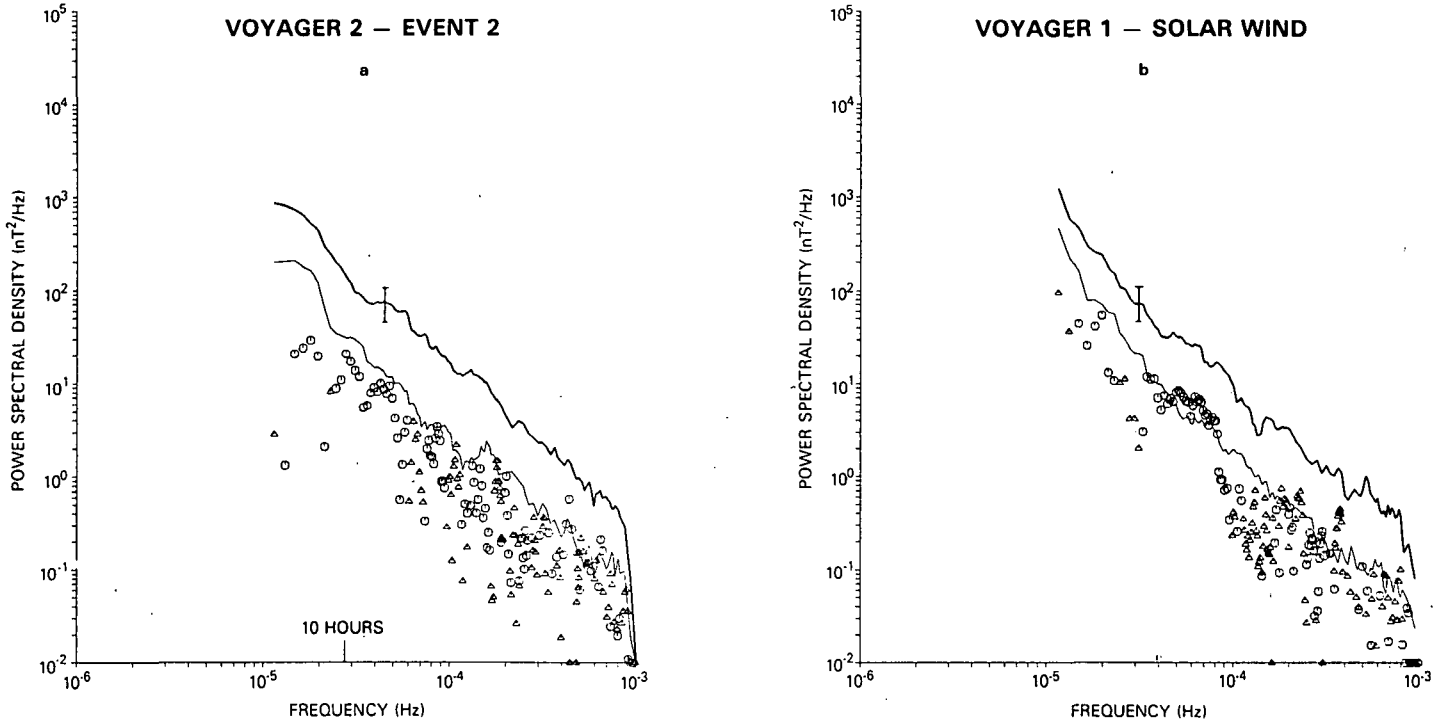

Figure 11

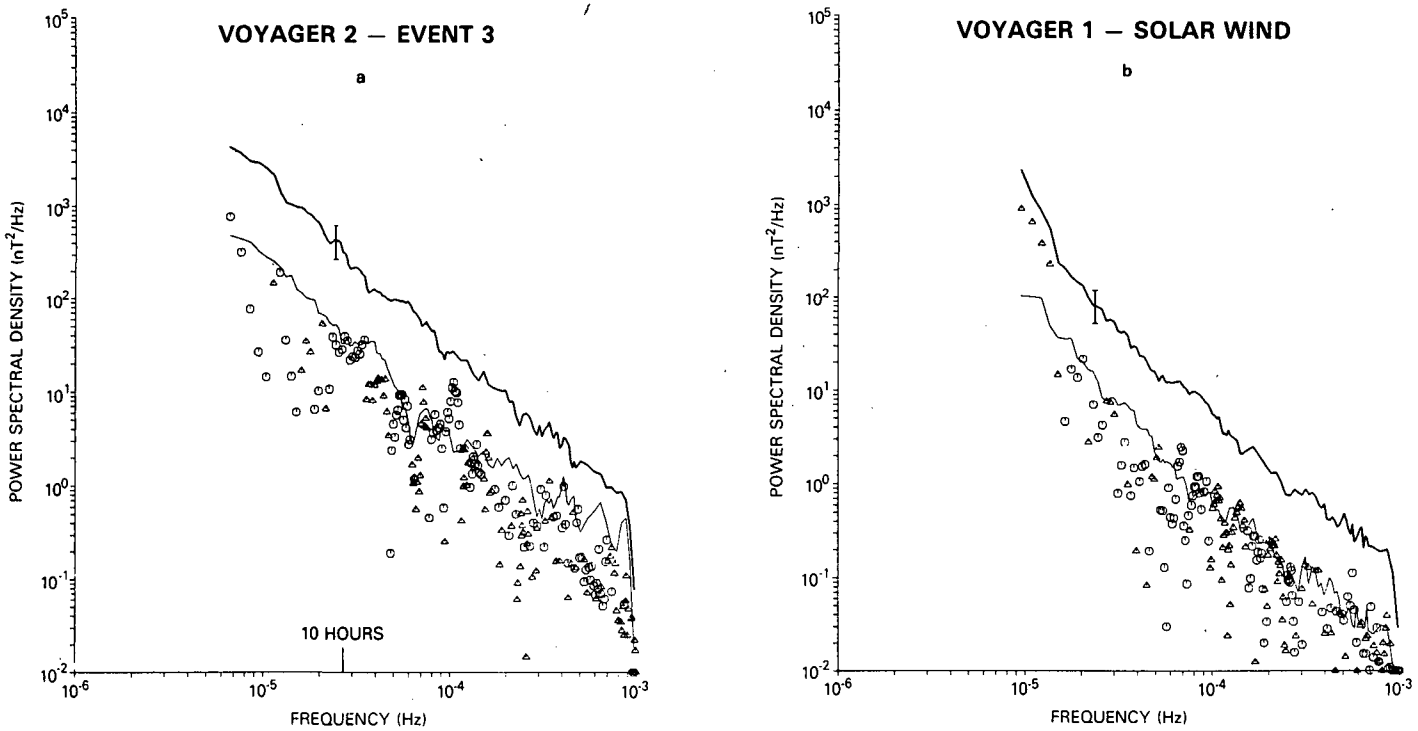
VOYAGER 2 — EVENT 3
a
VOYAGER 1 — SOLAR WIND
b
POWER SPECTRAL DENSITY (nT²/Hz)
FREQUENCY (Hz)
10 HOURS

Figure 12

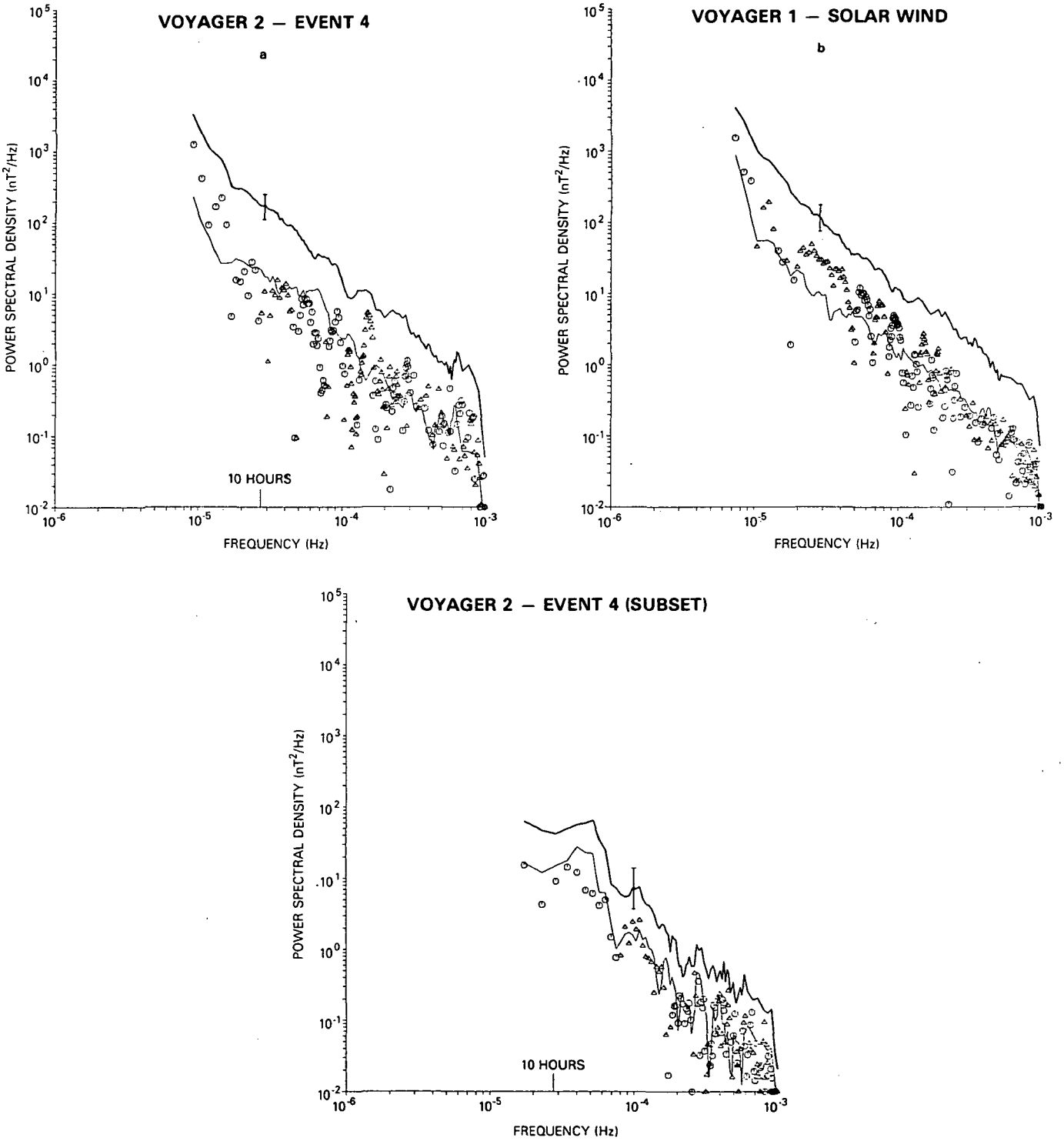

Figure 13

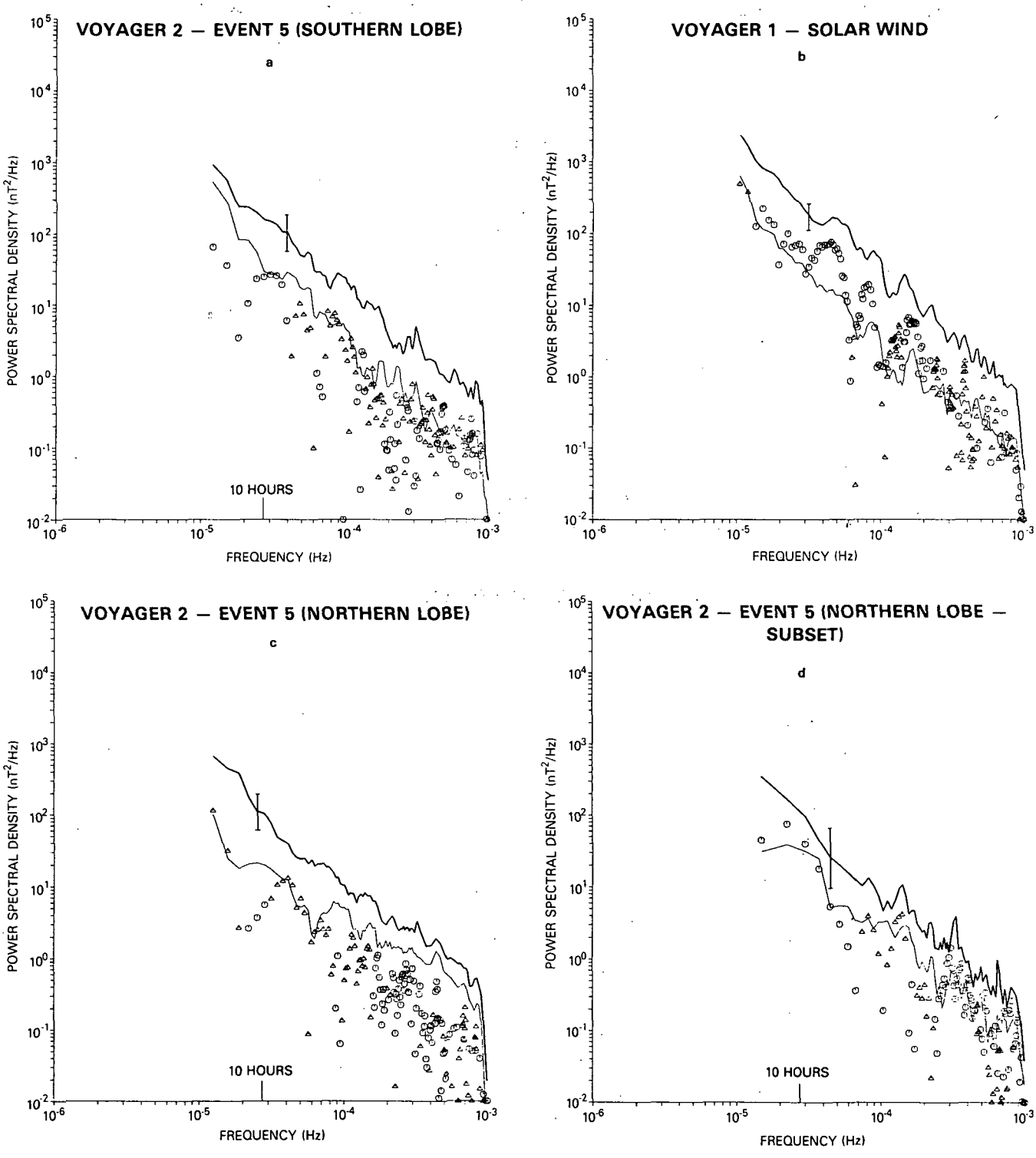
VOYAGER 2 — EVENT 5 (SOUTHERN LOBE)
a
VOYAGER 1 — SOLAR WIND
b
VOYAGER 2 — EVENT 5 (NORTHERN LOBE)
c
VOYAGER 2 — EVENT 5 (NORTHERN LOBE — SUBSET)
d
POWER SPECTRAL DENSITY (nT²/Hz)
FREQUENCY (Hz)
10 HOURS

Figure 14

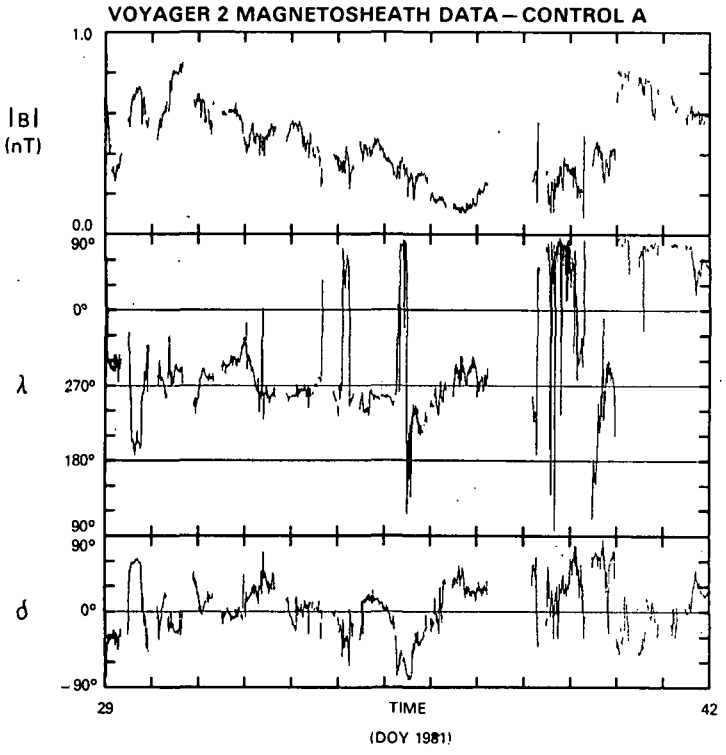

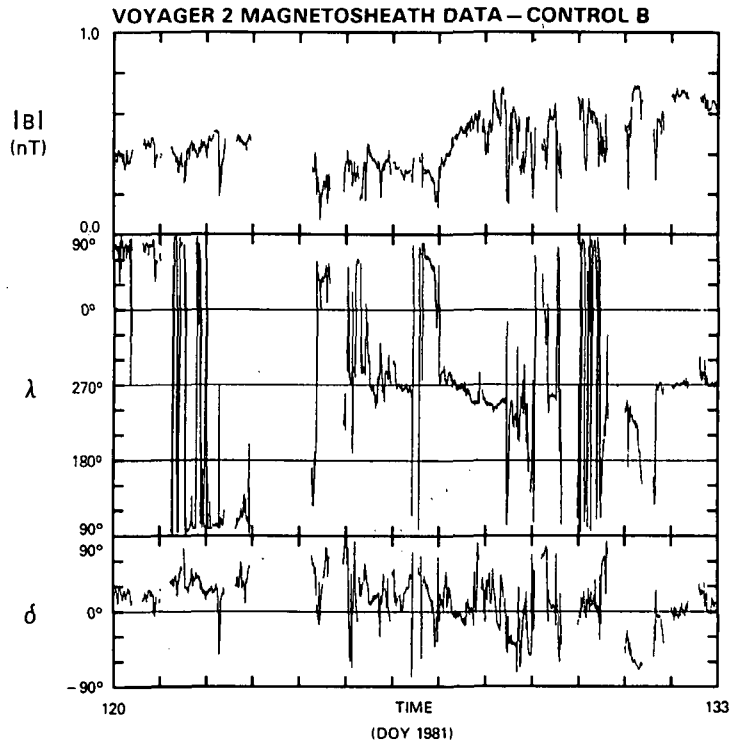

Figure 15

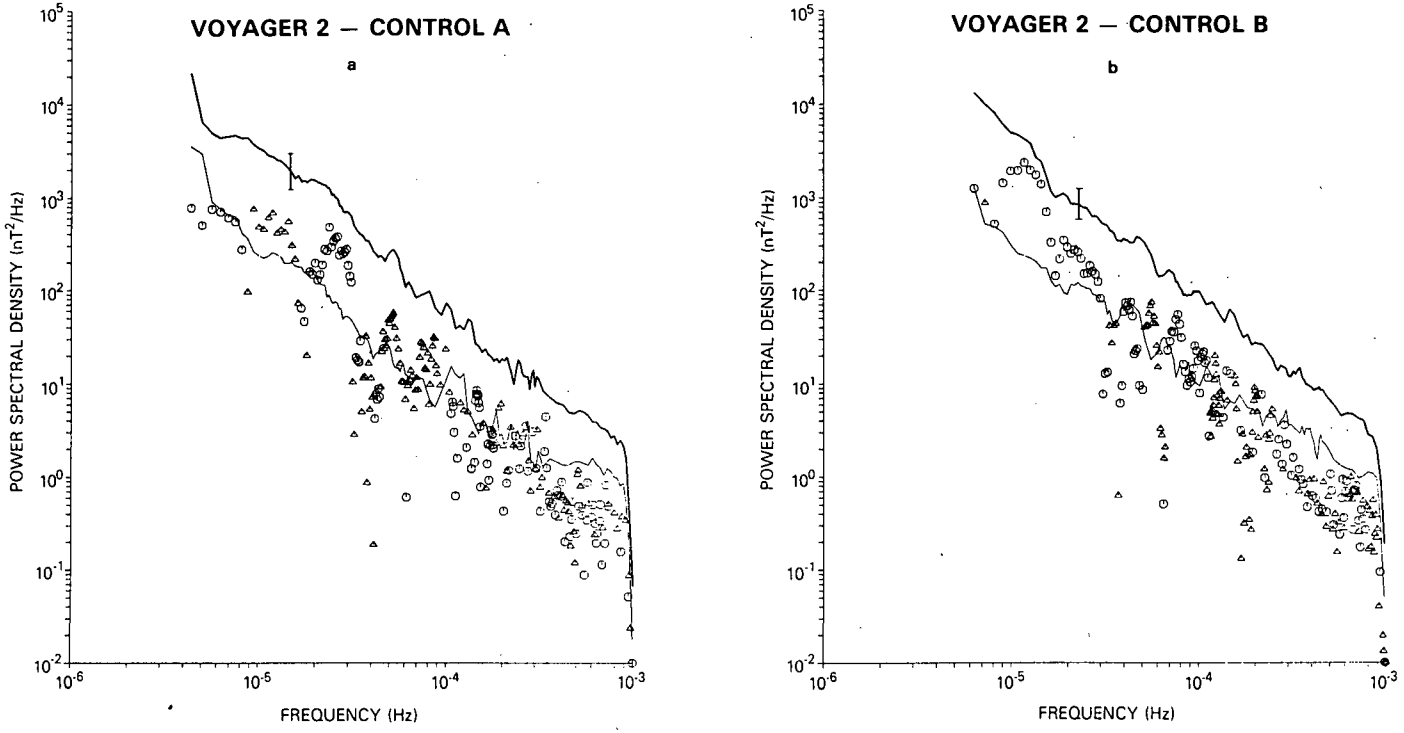
VOYAGER 2 — CONTROL A
a
VOYAGER 2 — CONTROL B
b
POWER SPECTRAL DENSITY (nT²/Hz)
FREQUENCY (Hz)
10⁵
10⁴
10³
10²
10¹
10⁰
10⁻¹
10⁻²
10⁻⁶
10⁻⁵
10⁻⁴
10⁻³

Figure 16

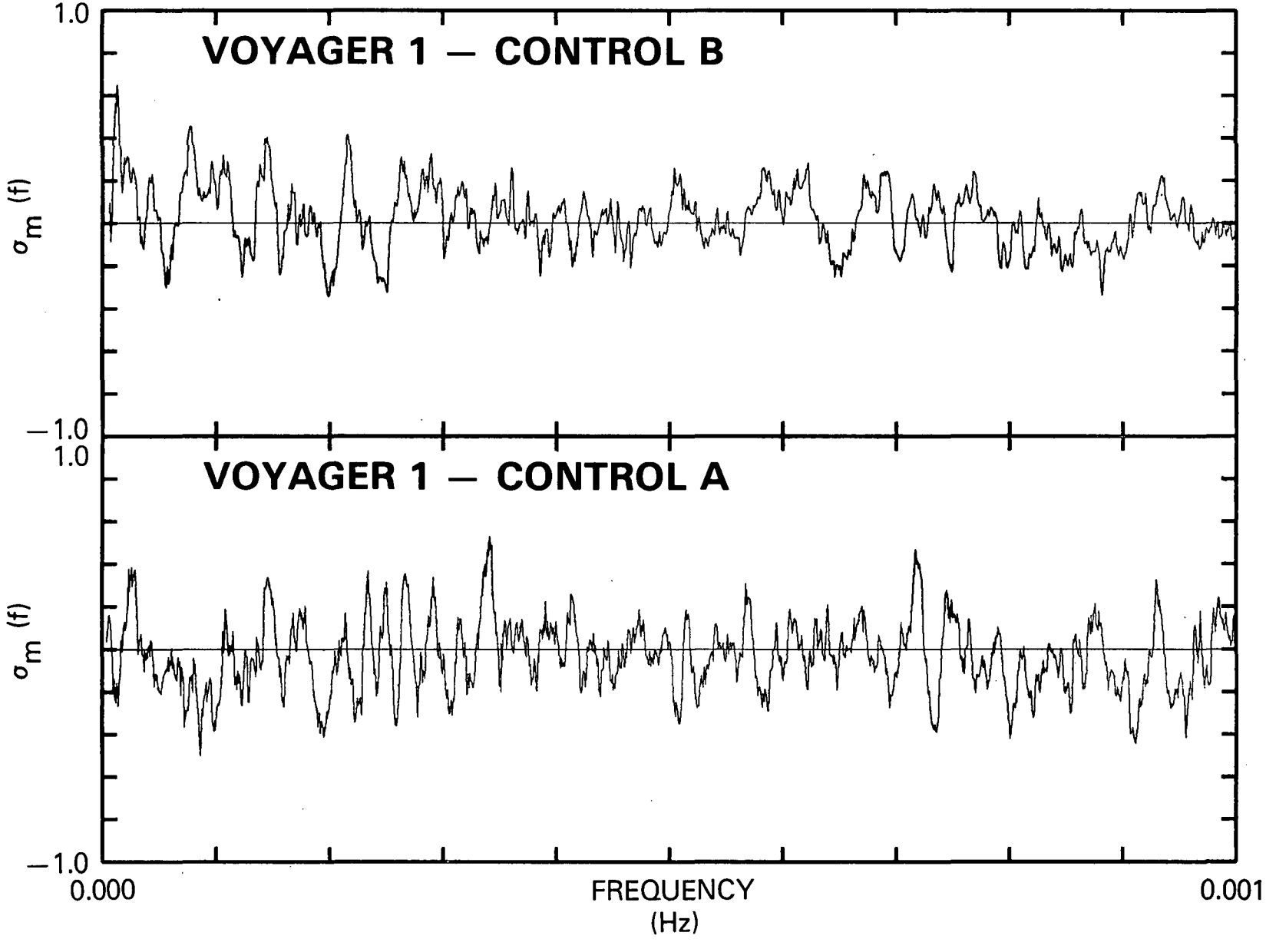
VOYAGER 1 — CONTROL B
VOYAGER 1 — CONTROL A
1.0
−1.0
σ_m (f)
0.000
FREQUENCY
(Hz)
0.001

Figure 17

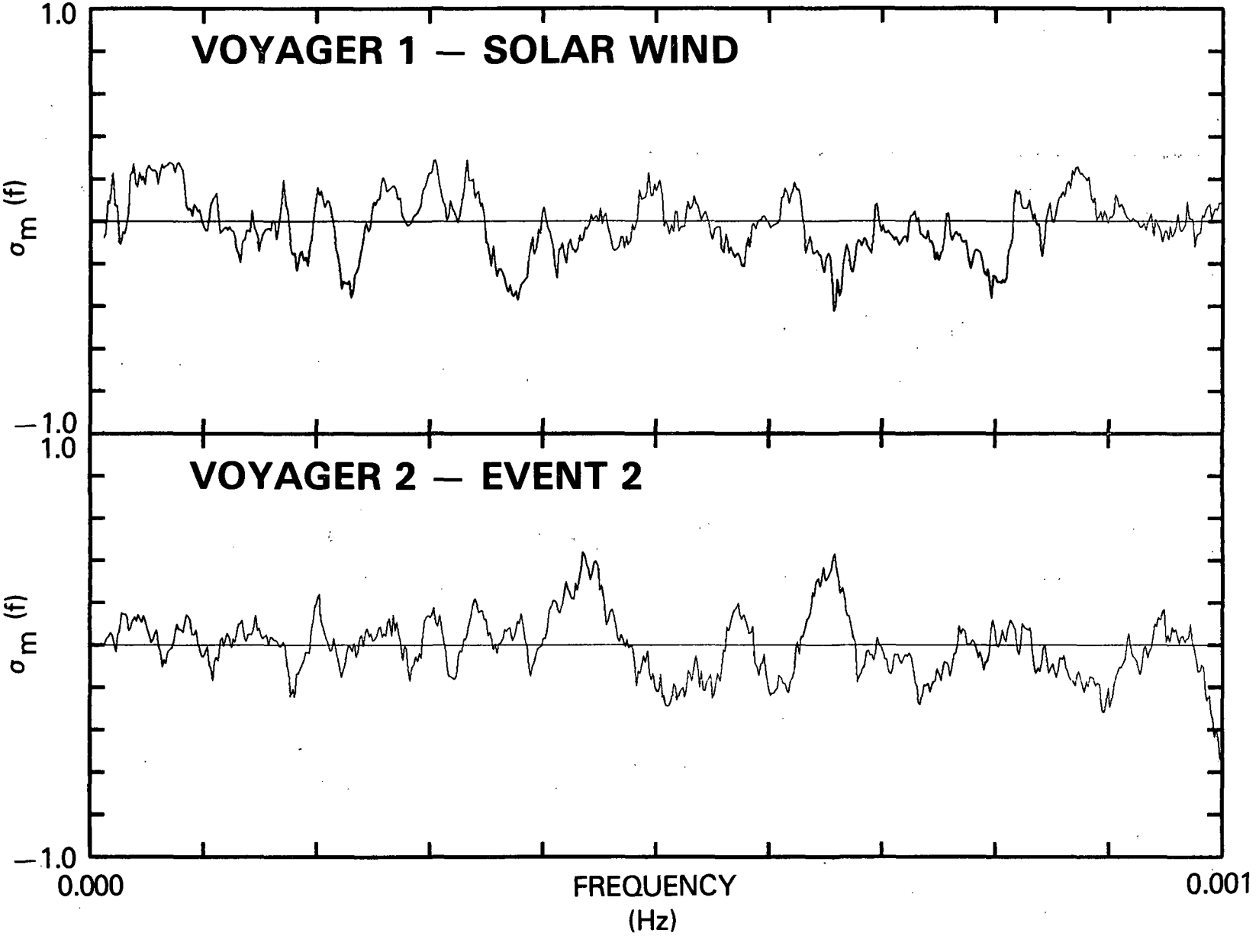
VOYAGER 1 — SOLAR WIND
VOYAGER 2 — EVENT 2
1.0
−1.0
1.0
−1.0
σm (f)
σm (f)
0.000
FREQUENCY
(Hz)
0.001

Figure 18

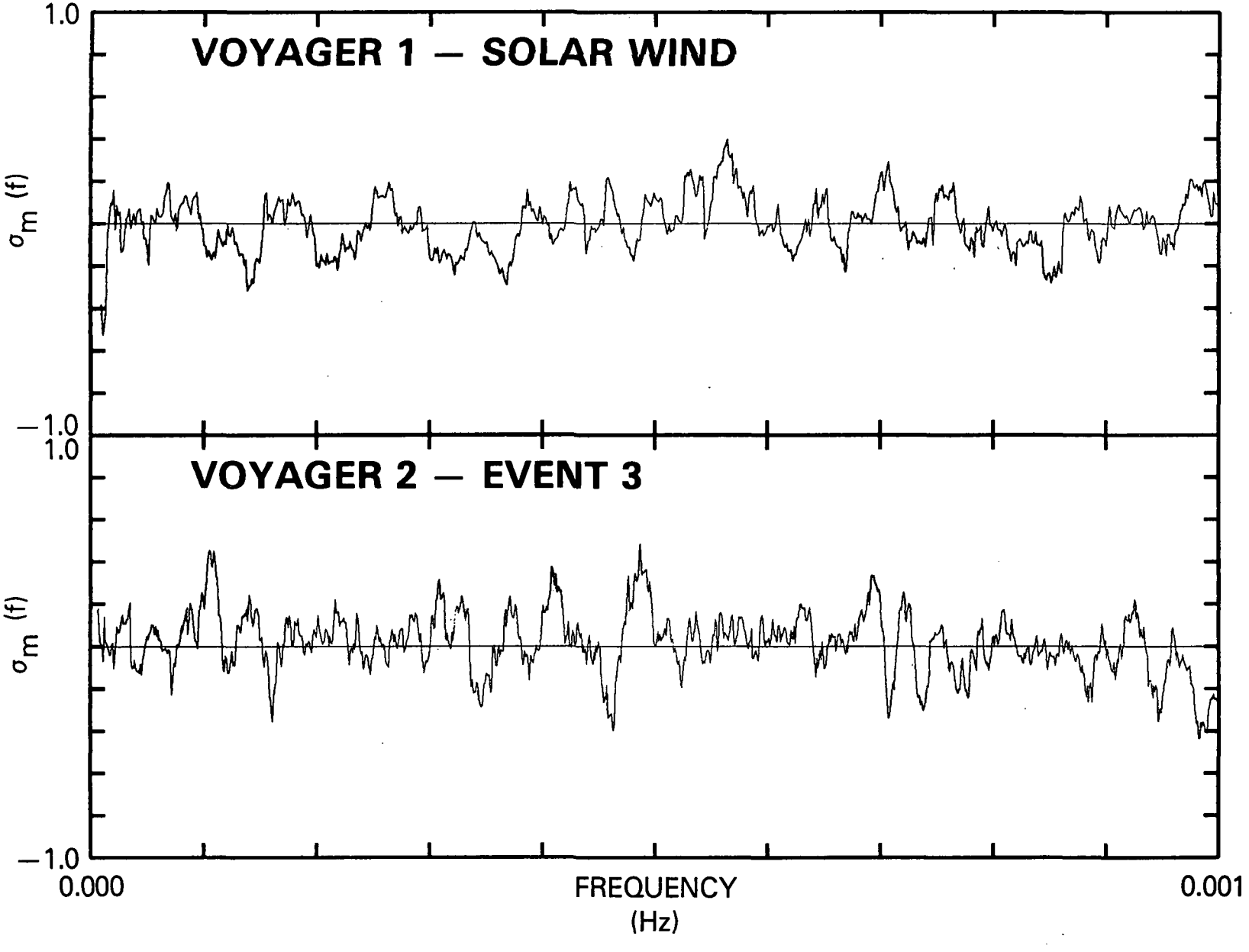
VOYAGER 1 — SOLAR WIND
VOYAGER 2 — EVENT 3
1.0
−1.0
σ_m (f)
0.000
FREQUENCY
(Hz)
0.001

Figure 19

BIBLIOGRAPHIC DATA SHEET

1. Report No.	2. Government Accession No.	3. Recipient's Catalog No.
TM 86159		

4. Title and Subtitle	5. Report Date
Magnetic Properties of Jupiter's Tail at Distances from 80-7500 Jovian Radii	September 1984
	6. Performing Organization Code
7. Author(s) M. L. Goldstein, R. P. Lepping and E. C. Sittler, Jr.	8. Performing Organization Report No.
9. Performing Organization Name and Address NASA/GSFC Laboratory for Extraterrestrial Physics Interplanetary Physics Branch, Code 692 Greenbelt, MD 20771	10. Work Unit No.
	11. Contract or Grant No.
	13. Type of Report and Period Covered Technical Memorandum
12. Sponsoring Agency Name and Address	14. Sponsoring Agency Code

15. Supplementary Notes

16. Abstract

SEE ATTACHED.

17. Key Words (Selected by Author(s))	18. Distribution Statement
Jupiter, magnetospheric structure, turbulence	

19. Security Classif. (of this report)	20. Security Classif. (of this page)	21. No. of Pages	22. Price*
U	U	64	

*For sale by the National Technical Information Service, Springfield, Virginia

GSFC 25-44 (10/77)